ACS Infectious Diseases

pubs.acs.org/journal/aidcbc

Article

Discovery of Amphamide, a Drug Candidate for the Second Generation of Polyene Antibiotics

Anna N. Tevyashova,* Elena N. Bychkova, Svetlana E. Solovieva, George V. Zatonsky, Natalia E. Grammatikova, Elena B. Isakova, Elena P. Mirchink, Ivan D. Treshchalin, Eleonora R. Pereverzeva, Evgeny E. Bykov, Svetlana S. Efimova, Olga S. Ostroumova, and Andrey E. Shchekotikhin

Cite This: *ACS Infect. Dis.* 2020, 6, 2029−2044

Read Online

ACCESS | Metrics & More | Article Recommendations | Supporting Information

ABSTRACT: Amphotericin B (AmB, **1**) is the drug of choice for treating the most serious systemic fungal or protozoan infections. Nevertheless, its application is limited by low solubility in aqueous media and serious side effects such as infusion-related reactions, hemolytic toxicity, and nephrotoxicity. Owing to these limitations, it is essential to search for the polyene derivatives with better chemotherapeutic properties. With the objective of obtaining AmB derivatives with lower self-aggregation and improved solubility, we synthesized a series of amides of AmB bearing an additional basic group in the introduced residue. The screening of antifungal activity in vitro revealed that *N*-(2-aminoethyl)amide of AmB (amphamide, **6**) had superior antifungal activity compared to that of the paternal AmB. Preclinical studies in mice confirmed that compound **6** had a much lower acute toxicity and higher antifungal efficacy in the model of mice candidosis sepsis compared with that of AmB (**1**). Thus, the discovered amphamide is a promising drug candidate for the second generation of polyene antibiotics and is also prospective for in-depth preclinical and clinical evaluation.

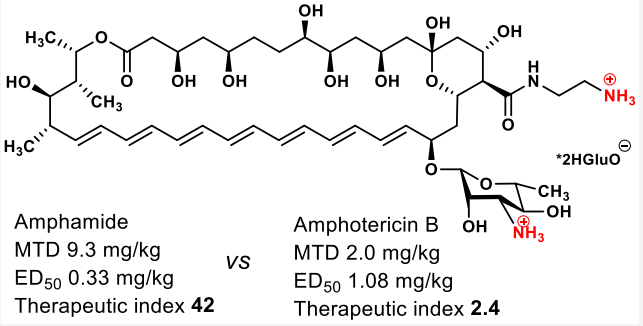

KEYWORDS: *polyene antibiotics, amphotericin B, antifungal activity, acute toxicity, in vivo antifungal efficacy, mechanism of action*

Fungal infections affect more than 1 billion people and result in approximately 11.5 million life-threatening infections and more than 1.5 million deaths annually.[1,2] Thus, immunocompromised hosts (e.g., patients suffering from AIDS or hematological diseases, transplant recipients, and those under critical care or chemotherapy) are especially vulnerable to fungal infections, and the rates of mortality and morbidity in cases of invasive fungal diseases are very high. Furthermore, because risk factors for immune failure continue to increase in frequency, the incidence of systemic mycoses will most likely continue to increase. Despite over six decades of clinical use, AmB (**1**, Figure 1) is the gold standard for antifungal treatment for the most severe fungal infections, because it has a broad spectrum of antifungal activity, and clinically significant drug resistance to it is very rare. Nevertheless, the application of AmB is limited by its low solubility in aqueous media and by serious side-effects such as infusion-related reactions, hemolytic toxicity, and nephrotoxicity.[3] Therefore, it is imperative to search for new polyene derivatives with better chemotherapeutic properties.[4]

The mechanism of action of antifungal polyenes has been studied for a long time but still remains controversial. The first described mode of action was pore formation after binding to sterols that are present in the cell membrane.[5−7] The

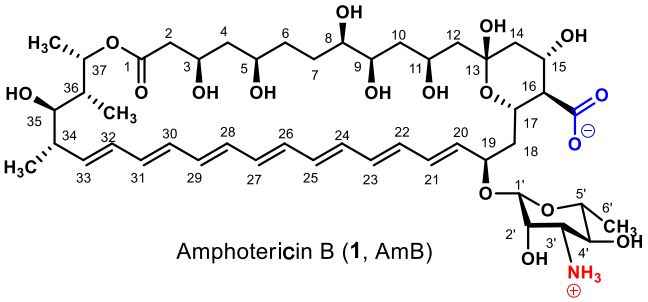

Figure 1. Structures of polyene antibiotic amphotericin B.

selectivity of AmB binding to ergosterol (ERG) compared to that of cholesterol (CHOL) results in its greater activity toward fungal cells than toward mammalian cells, which

Received: February 12, 2020
Published: June 29, 2020

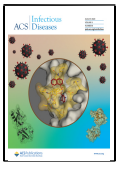

https://dx.doi.org/10.1021/acsinfecdis.0c00068
ACS Infect. Dis. 2020, 6, 2029−2044

Scheme 1. Synthesis of AmB Derivatives 2−10

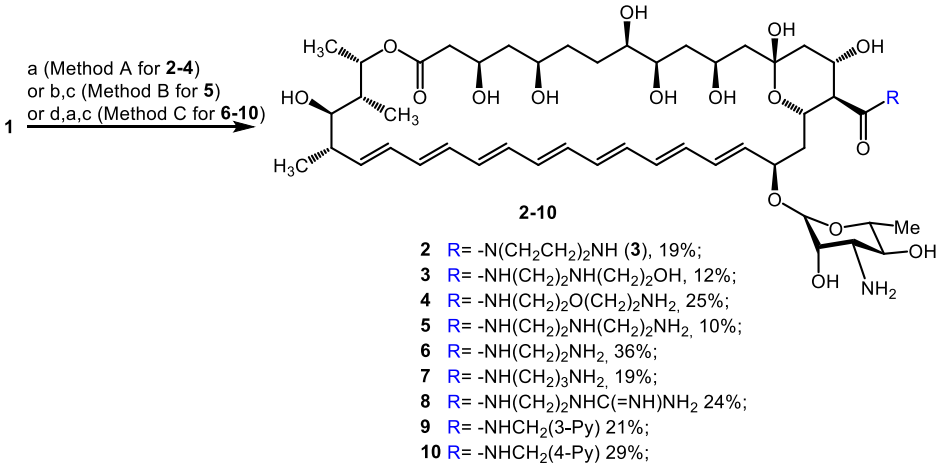

a) amine, PyBOP, Et_3N, DMSO; b) $NH_2CH_2CH_2N(Fmoc)CH_2CH_2NH_2$*TFA, PyBOP, Et_3N, DMSO; c) piperidine, DMSO-MeOH (3:1); d) Fmoc-OSu, Py, DMF-MeOH (5:1).

enables its therapeutic use. This need for sterol has been used as a guiding idea in the attempts to design derivatives that are more selective to ERG-containing fungal membranes than to CHOL-rich mammalian membranes, which decreases the AmB side effects. However, some investigations have demonstrated that the role of sterols in the formation of the AmB-formed channel is related to the effects they have on the structure of the membrane itself rather than to the direct involvement in the channel formation.[8] Later investigations have revealed that AmB affects fungal cells via the induction of oxidative stress.[9,10] Recently, a sponge model, which suggests that AmB forms clusters that extract sterols from cell membranes, has been proposed.[11,12]

Previous studies have demonstrated that the selectivity of AmB toward fungal membranes is linked to its self-association properties.[13] Presumably, AmB oligomers that formed prior to membrane insertion act differently on fungal (ERG-rich) and mammalian (CHOL-rich) membranes.[14] It has been shown that regardless of the AmB form (i.e., monomeric or aggregated), AmB can form ion channels in ERG-containing phosphatidylcholine bilayer model membranes.[15] However, AmB cannot form ion channels in its monomeric form in sterol-free and CHOL-containing membranes.[15] This is the possible explanation for the lower toxicity of solutions in which AmB is almost entirely monomeric compared to the corresponding solutions of the drug formulation Fungizone in which the polyene is present in an almost completely self-aggregated form.[16] Recently, based on the hypothesis that there is a need for antibiotic dimerization for the appearance of ion channels in CHOL-containing membranes,[15] a series of C-16 derivatives has been designed.[17] A new potent AmB derivative (carboxamide of AmB and L-histidine methyl ester) with improved safety owing to its decreased dimerization in solution has been discovered.[17] Thus, the reduction of dimerization properties of AmB derivatives is the approach that can lead to a more selective and less toxic antifungal agents. Thereby, we synthesized a series of AmB derivatives with presumably reduced aggregation properties. Because the ionic state (net electrical charge) of polyene antibiotics is the major factor that determines their aggregation and solubility properties,[18] we designed a series of C16-carboxamides of AmB containing a basic group that can be protonated and cause reduced aggregation in aqueous solutions as well as improved water solubility. Our previous study on the series of semisynthetic derivatives of genetically engineered polyene antibiotics (29-didehydronystatin A1 (S44HP), BSG005) revealed that the introduction of a side chain with a tertiary amino group on the amide moiety led to the improvement in water solubility and in some cases to an increase in the antifungal activity of semisynthetic analogs.[19−21] It has been also determined that the alkylation of the mycosamine moiety of AmB (**1**) with two aminopropyl groups also leads to congeners with significantly increased antifungal activity, including that against the AmB-resistant strain.[22]

However, the introduction of the positively charged group at the C16 position also disturbs the zwitterionic interaction between C16-carboxylic and amino groups (Figure 1) in the mycosamine moiety that charge the polyene core conformation and force the sugar ring toward the membrane. The mycosamine appendage is known to be essential in promoting the AmB-ERG binding interaction, which is essential for the antifungal activity. Recently, new less toxic ureides of AmB have been described.[23] These derivatives demonstrated a considerably lower toxicity, which can be explained by the introduction of the protonated nitrogen atom between the C16 and the carboxylic carbons that perturb the putative intramolecular salt bridge interaction and thereby favor ERG over CHOL binding.[23]

Herein, we report the synthesis and studies of the antifungal activity of C16-modified AmB derivatives, which led to the discovery of the drug candidate amphamide, which is more potent than paternal antibiotic in vitro and has increased efficiency and improved safety. In addition, the chosen drug candidate was subjected to electrophysiological and pharmacological studies. It was determined that amphamide has a much lower acute toxicity and higher antifungal efficiency in the model of mice candidosis sepsis compared with those of AmB presumably due its lower self-aggregation properties.

RESULTS

Chemistry. To disturb the zwitterionic interaction and increase solubility and steric effects between the introduced amide moiety and mycosamine residue of AmB, a new series of derivatives obtained by the transformation of C16-carboxylic

https://dx.doi.org/10.1021/acsinfecdis.0c00068
ACS Infect. Dis. 2020, 6, 2029−2044

Table 1. Antifungal Activity of the Semisynthetic AmB Derivatives 2−10 in Comparison with AmB (1)

	Minimum Inhibitory Concentration (MIC, μg/mL)[a]											
	C.albicans ATCC 24433		*C.parapsilosis* ATCC 22019		*C. krusei* 432M		*C. tropicalis* 3019		*C. glabrata* 61L			
compound	24 h	48 h	24 h	48 h	24 h	48 h	24 h	48 h	24 h	48 h	*M. canis* B-200	*T. rubrum* 2002
AmB (1)	0.125	0.25	0.25	0.5	0.25	0.5	0.06	0.25	0.06	0.25	0.25	0.25
2	0.25	0.5	0.25	0.5	4	4−8	1	2	0.25	1	1−2	2
3	0.03	0.06	0.06	0.125	0.25	0.5	0.125	0.125	0.06	0.125	0.125	0.25
4	0.06	0.25	0.25	0.5	1	2	0.125	0.5	0.125	0.5	1	0.5
5	0.125	0.25	0.125	0.25	0.5	1.0	0.125	0.25	0.125	0.25	0.5	0.25
6 (amphamide)	0.03	0.06	0.03	0.06	0.125	0.25	0.03	0.06	0.03	0.06	0.5	0.5
6G	0.03	0.06	0.03	0.06	0.125	0.25	0.03	0.06	0.03	0.06	0.5	0.5
7	0.25	0.5	0.25	0.5	2	4	0.125	0.5	0.125	0.5	1	0.5
8	>32	>32	>32	>32	>32	>32	>32	>32	>32	>32	>32	>32
9	0.06	0.125	0.125	0.5	0.25	0.5	0.125	0.25	0.125	0.25	0.25	0.25
10	0.125	0.25	0.25	0.5	0.25	1.0	0.25	0.5	0.125	0.25	0.25	0.5

[a]MICs are measured as the lowest concentration of agents that prevent any visible growth. The results of the experiments were definitely reproducible. In cases of full coincidence of the data obtained, the MIC is represented as a single number.

group into carboxamide was prepared. A set of amines bearing additional amino groups as well as strongly basic (guanidine) or low basicity (pyridine) residues were used to achieve the amidation of AmB. The commercially unavailable starting derivatives (9*H*-fluoren-9-yl)methyl bis(2-aminoethyl)-carbamate trifluoroacetate and 1-(2-aminoethyl)guanidine were obtained from (9*H*-fluoren-9-yl)methyl bis(2-((*tert*-butoxycarbonyl)amino)ethyl)carbamate and *N*-Boc-ethylenediamine hydrochloride, respectively (see the Methods section for details).

Three synthetic approaches were used for the preparation of target AmB amides. The first one included the direct amidation of the C16-carboxylic group by the corresponding amine in the presence of benzotriazol-1-yl-oxytripyrrolidinophosphonium hexafluorophosphate (PyBOP) and the subsequent purification of the obtained AmB-amide by column chromatography (Method A). *N*-(2-((2-Aminoethyl)amino)ethyl)amide of AmB (**5**) was obtained from AmB (**1**) and (9*H*-fluoren-9-yl)methyl bis(2-aminoethyl)carbamate trifluoroacetate in two steps: amidation of the C16-carboxylic group with *N*-Fmoc-protected amine and subsequent deprotection of the secondary amino group (Method B, Scheme 1). The intermediate Fmoc-protected amide (**Fmoc-5**) was purified by column chromatography. Finally, the Fmoc-protected AmB (**Fmoc-1**) was applied when the attempt to purify target amides obtained by the direct amidation of AmB was unsuccessful because it prevents side reactions, improves solubility of the derivatives in organic solvents, and facilitates the column chromatography purification procedure (Method C).

Using the first approach, AmB (**1**) was amidated by the excess of 1,4-piperazine, *N*-(2-hydroxyethyl)ethylenediamine, or 2,2′-oxidiethanamine in the presence of PyBOP in DMSO. Crude products were purified by column chromatography and produced 1-(piperazin-1-yl)-, *N*-(2-((2-hydroxyethyl)amino)-ethyl)- and *N*-(2-(2-aminoethoxy)ethyl)-amides of AmB **2−4** (Method A, Scheme 1). *N*-(2-((2-Aminoethyl)amino)ethyl)-amide of AmB (**5**) was obtained from AmB (**1**) and (9*H*-fluoren-9-yl)methyl bis(2-aminoethyl)carbamate trifluoroacetate in two steps: amidation of the C16-carboxylic group with *N*-Fmoc-protected amine and subsequent deprotection of the secondary amino group (Method B, Scheme 1). The intermediate Fmoc-protected amide (**Fmoc-5**) was purified by column chromatography.

The other synthetic sequence for AmB amides **6−10** included blocking of the amino group of AmB with the Fmoc-protective group, amidation of the obtained *N*-Fmoc-AmB (**Fmoc-1**) with ethylenediamine, 1,3-diaminopropane, 1-(2-aminoethyl)guanidine, 3-picolylamine, or 4-picolylamine, purification of the Fmoc protected amides by column chromatography, and deprotection of the amino group (Method C, Scheme 1). The yields of the target amides **2−10** varied from low to moderate (10−41%) due to well-known high lability of polyene antibiotics, their sensitivity to light and oxygen, and basic/acid conditions. In general, the yields of amides **6−10** obtained via the *N*-Fmoc-AmB intermediate (**Fmoc-1**, Method C) were higher (19−36%, total yield) compared to those of amides **2−5** obtained by the direct amidation of AmB (**1**) (Scheme 1) (10−25%). Thus, the use on the Fmoc protective group was favorable for the synthesis of AmB derivatives, because it simplified the chromatographic purification by increasing the solubility of intermediate compounds and decreasing the irreversible adsorption of AmB derivatives on silica gel.

The purity of new amides **2−10** was determined by TLC and HPLC, and the structure was confirmed by HR-ESI mass spectrometry and NMR spectra. To fully assign signals in both ^{1}H and ^{13}C spectra, a set of 2D experiments was performed: ^{1}H−^{1}H COSY, TOCSY, NOESY (ROESY), HSQC, HMBC, and H2BC.[24] The latter experiment was especially useful to assign resonances from the polyene part of molecules. In addition, a set of selective TOCSY experiments was performed aiming to assign the polyene part from H-19, H-20, H-33, and H-34 resonances. The assignment of ^{1}H and ^{13}C signals for compounds **2−10** is shown in Table S1 (Supporting Information).

In Vitro Antifungal Activity. The antifungal activity of AmB derivatives **2−10** was tested against the strains of *Candida spp.* (*C. albicans* ATCC 24433, *C. krusei* 432M, *C. tropicalis* 3019, *C. glabrata* 61L) and filamentous fungus (*M. canis* B-200, *T. rubrum* 2002) and compared to that of AmB (**1**) using the broth microdilution method, as described in the NCCLS documents M27-A[25] and M38-A[26] (Table 1). Reference strain *C. parapsilopsis* ATCC 22019 was used as

https://dx.doi.org/10.1021/acsinfecdis.0c00068
ACS Infect. Dis. 2020, 6, 2029−2044

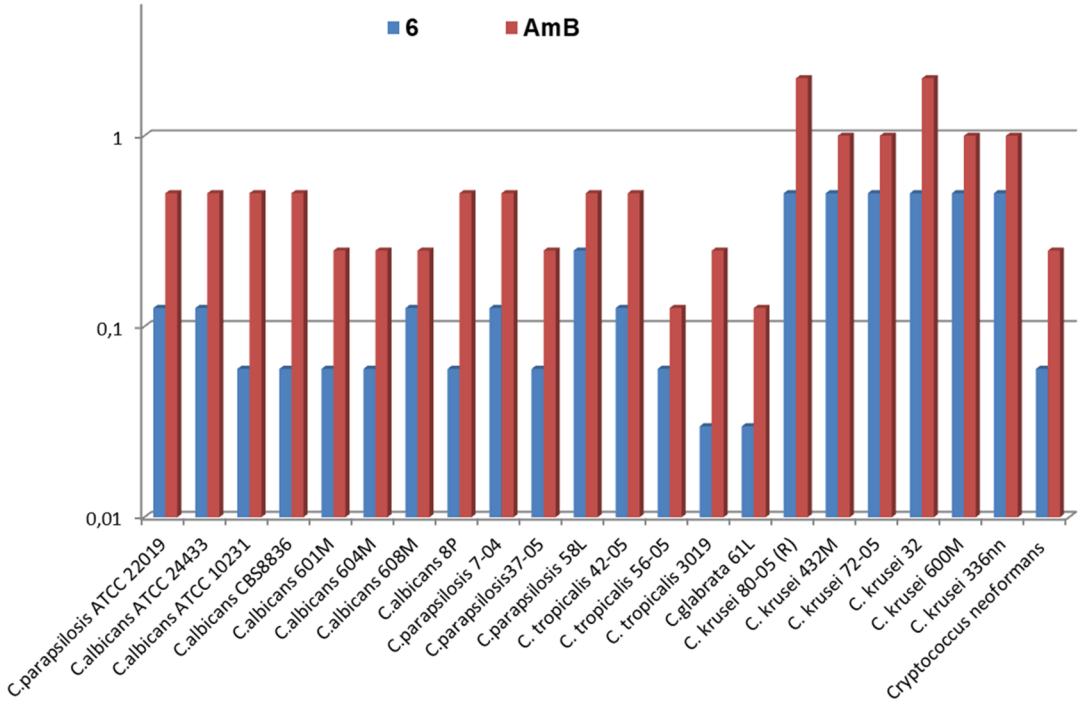

Figure 2. In vitro antifungal activity (MIC, μg/mL, after 24 h) for the compound **6** in comparison with AmB (**1**).

the control in each experiment. In all experiments, the in vitro microdilution technique in 96-microwell plates was applied. The minimum inhibitory concentration (MIC) was defined as the lowest concentration that resulted in complete growth inhibition after incubation for 24 and 48 h for *Candida spp*. and 48−72 h for dermatophytes.

Amides **2**−**7** and **9**−**10** demonstrated high antifungal activity against tested *Candida* and filamentous fungus strains (Table 1). In general, amides **2**, **4**, and **7** were approximately two times less active (MICs values ∼0.125−8 μg/mL) than parent AmB (MICs values ∼0.06−0.5 μg/mL). Compounds **3**, **4**, and **9** demonstrated higher than or equal to AmB antifungal activity against tested strains, while compound **6** demonstrated higher antifungal potency than that of parent AmB (**1**) against all tested *Candida* and filamentous fungus strains. *N*-(2-Aminoethyl)amide of AmB (**6**) has moderate solubility in water. However, we observed that its L-glutamate salt (**6G**) was stable and soluble in water. Moreover, **6G** has in vitro antifungal activity that is similar to that of the free base form of **6** (Table 1). The increase in the length of the alkyl spacer between C16-amide and amino groups (compound **7**) resulted in a decrease in the antifungal activity (Table 1). Thereby, the amidation of the C16-carboxylic group of AmB with ethylenediamine (compound **6**) was determined to be favorable for increasing the antifungal activity of the antibiotic and for improving its solubility in an aqueous media. An addition of 2-hydroxyethyl- or 2-aminoethyl- residues into amide **6** resulted in the reduction of the antifungal activity (Table 1, compounds **3** and **5** vs compound **6**). The "shift" of the amino group by the insertion of the ethoxyethyl spacer resulted in the reduction of the antifungal activity (Table 1, compound **4** vs compound **6**).

Picolylamides (**9**, **10**) bearing weakly basic pyridine residues were also less active than the most active compound **6**. However, the antifungal activity of 3-picolylamide **9** was similar to that of AmB (**1**), and 3-picolylamide **9** was two times more active than 4-picolylamide **10** (Table 1). The introduction of the strongly basic guanidine residue in amide (compound **8**) resulted in a total loss of the antifungal activity, i.e., the MICs values for corresponding amide **8** were >32 μg/mL against all tested strains. Thus, it was demonstrated that the introduction of small amino or alkylamino groups or a weakly basic pyridine residue into carboxamide AmB is advantageous for the antifungal activity and increases the size of the side chain; the introduction of strongly basic (guanidine) or several polar groups (amino or hydroxyl) was less favorable for the antifungal activity.

The antifungal activity of **6**, which we called amphamide, was additionally tested on a wide panel of *Candida spp*. including ATCC strains and clinical isolates (Figure 2) (MIC, μg/mL, after 24 h).

Amphamide (**6**) was at least two times more active than AmB (**1**) against all tested Candida stains; 4 times more active than AmB (**1**) against *C. parapsilosis* ATCC 22019, *C. albicans* ATCC 24433, *C. albicans* CBS8836, *C. albicans* 601M, *C. albicans* 604M, *C. albicans* ATCC 10231, *C. parapsilosis* 7-04, *C. parapsilosis* 37-05, *C. tropicalis* 42-05, *C. glabrata* 61L, *C. krusei* 80-05(R), *C. krusei* 32, *Cryptococcus neoformans*; 8 times more active than AmB against*C. albicans* 8P, *C. tropicalis* 3019 (Figure 2).

Based on the in vitro antifungal data, amphamide (**6**) was selected for further in-depth investigations and preclinical evaluation.

Spectroscopic Experiments. As an additional advantage of the amphamide **6G** is its increased solubility in water, we also checked its aggregation behavior in an aqueous solution. An estimate of polyene aggregation can be obtained from the ratio between the absorbance at a wavelength of 409 nm and the corresponding one at a wavelength of 347 nm. The first wavelength is characteristic of a monomeric state of the polyene, whereas aggregation produces absorbance at the second wavelength.[17] Figure 3A presents the UV spectra

https://dx.doi.org/10.1021/acsinfecdis.0c00068
ACS Infect. Dis. 2020, 6, 2029−2044

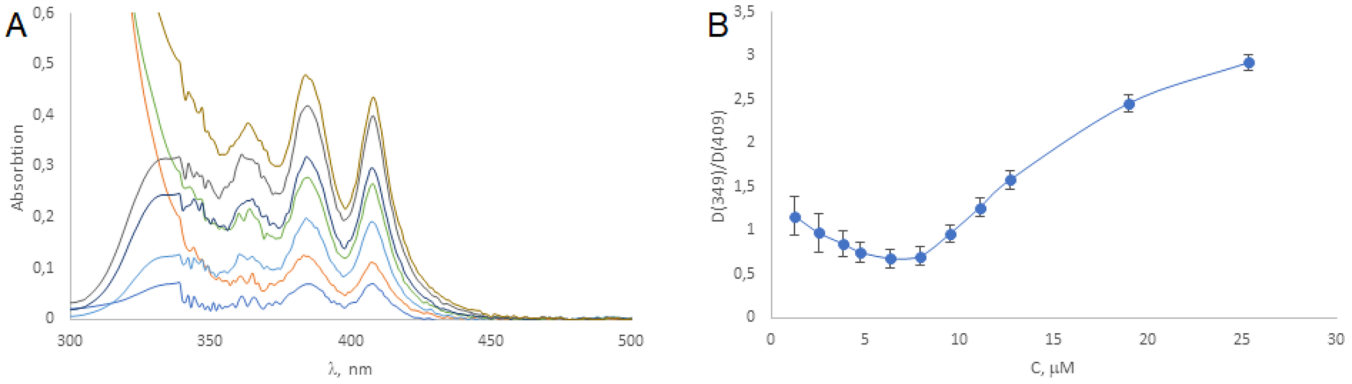

Figure 3. (A) Absorption spectra in a PBS solution at 20 °C of different concentrations of the compound **6G**. (B) Ratio between absorbance at 347 nm and that at 409 nm as a function of concentration of compound **6G**.

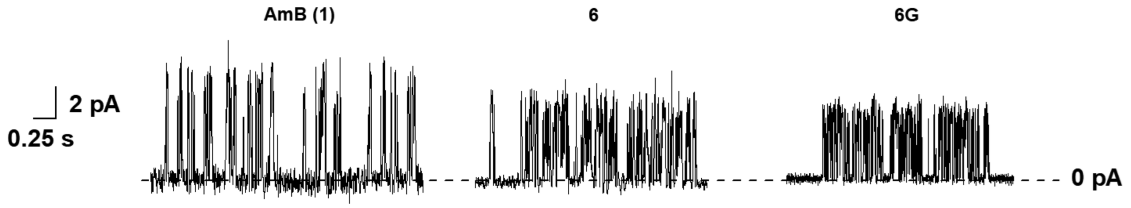

Figure 4. Current fluctuations corresponding to openings and closures of single channels induced by 0.9×10^{-7} M AmB (**1**), 0.7×10^{-7} M (**6**), and 0.4×10^{-7} M (**6G**). The lipid bilayers composed of DPhPC:ERG (67:33 mol %) and were bathed in 2.0 M KCl (pH 7.4). The transmembrane voltage was +200 mV.

corresponding to the compound **6G** as well as the profile of the ratio of absorbance at 347 nm/absorbance at 409 nm at different concentrations (Figure 3B).

The point where the ration D(347/409) start to increase corresponds to the beginning of the aggregation of molecules in the solution. Thus, the dimerization onset for compound **6G** was observed at concentration 6.3 μM/L. We failed to plot the range of UV spectra for AmB (**1**) because of its extremely low solubility in PBS solution, but previously described dimerization concentration for this antibiotic was in the range 0.2−1 μM/L;[17] thus, we can conclude that amphamide **6G** has 6 31-fold lower aggregation properties than the parent AmB (**1**).

Model Membrane Experiments. We ran a series of electrophysiological experiments to identify differences in the impact of cellular membrane models for AmB (**1**) and new derivative **6** and its water-soluble L-glutamate salt **6G**, which can explain the increased antifungal activity of amphamide.

Figure 4 shows current fluctuations corresponding to openings and closings of single channels formed by one-sided addition of AmB (**1**), **6**, and **6G** into lipid bilayers composed of DPhPC and ERG (67:33 mol %) in 2 M KCl (pH 7.4) at +200 mV. The tested polyenes **6** and **6G** produce pores with smaller amplitudes than those produced by AmB (**1**) under the same conditions.

Figure 5 shows the dependence of conductance of single-length polyene channels (G) produced by AmB (**1**) and its derivatives **6** and **6G** in DPhPC:ERG (67:33 mol %) bilayers on transmembrane voltage (V).

Table 2 summarizes the values of the mean conductance at +200 mV. The characteristic parameters of the membrane activity of different polyenes were the averages of 5 to 9 experiments (mean ± sd).

The conductance of polyene single-length channels at +200 mV increases in the order of **6G** < **6** < AmB (**1**) (Figure 5). It has been previously shown that the addition of polyene to one

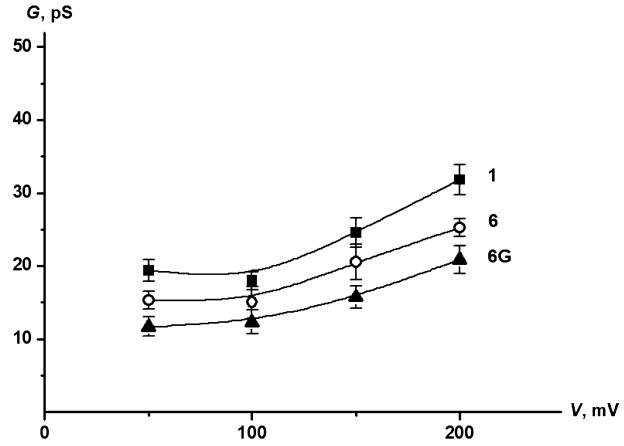

Figure 5. $G-V$ curves of single channels produced by AmB (**1**), **6**, and **6G**. Membranes were composed from DPhPC:ERG (67:33 mol %) and bathed in 2.0 M KCl (pH 7.4). The related polyene concentrations required to observe single pores induced by AmB (**1**), **6**, and **6G** are presented in a third column of Table 2.

side of the membrane leads to the formation of the asymmetric polyene/lipid pore.[27,28] This channel is characterized by predominant cationic selectivity and is predicted to have a wide entrance near the C15-(OH) funneling to its narrowest region near the C3-(OH) group.[29−33] For the anion−cation pair coordination in the half-pore, the cation is shifted toward the tail end of the pore. The anion ligand is C5-(OH), and the cation ligands are C3-(OH) and oxygen of the C1-carboxylic group. We did not observe any differences in the partial charges of oxygens in ligand C3-(OH) and C5-(OH)-groups of AmB (**1**), **6**, and **6G** calculated by the density functional method B3LYP/6-31G (d)[34] (Figure 6). Hence, in the case of compounds **6** and **6G** the observed changes in the conductances of the pores in comparison with AmB (**1**) is

https://dx.doi.org/10.1021/acsinfecdis.0c00068
ACS Infect. Dis. 2020, 6, 2029−2044

Table 2. Characteristic Parameters of the Membrane Activity of AmB Derivatives 6 and 6G Compared to That of AmB (1)

Polyene	C_{CHOL},[a] 10^{-7} M	C_{ERG},[b] 10^{-7} M	C_{CHOL}/C_{ERG}[c]	G_{+200},[d] pS	τ,[e] ms	P_{op}[f]	P_{So},[g] %
AmB (**1**)	2.4 ± 0.3	1.2 ± 0.3	2.0	31.7 ± 2.1	23 ± 4	0.49 ± 0.09	90 ± 7
6	2.2 ± 0.2	0.8 ± 0.1	2.9	25.2 ± 1.2	8 ± 1	0.26 ± 0.07	40 ± 9
6G	1.6 ± 0.2	0.5 ± 0.2	3.1	20.8 ± 1.8	6 ± 2	0.23 ± 0.07	15 ± 9

[a] C_{CHOL} – the antibiotic threshold concentration required to observe single polyene channels in planar lipid bilayers composed of DPhPC:CHOL (67:33 mol %). [b] C_{ERG} – the antibiotic threshold concentration required to observe single polyene channels in planar lipid bilayers composed of DPhPC:ERG (67:33 mol %). [c] C_{CHOL}/C_{ERG} – the ratio between antibiotic threshold concentrations required to observe single polyene channels in membranes composed of DPhPC:CHOL and DPhPC:ERG (67:33 mol %). [d] G_{+200} – the mean conductance of single polyene channels at +200 mV in DPhPC:ERG (67:33 mol %). [e] τ – the mean dwell time of polyene pores in DPhPC:ERG (67:33 mol %). [f] P_{op} – the probability of polyene channels to be open in DPhPC:ERG (67:33 mol %). [g] P_{So} – the percentage of POPC-liposomes with gel domains.

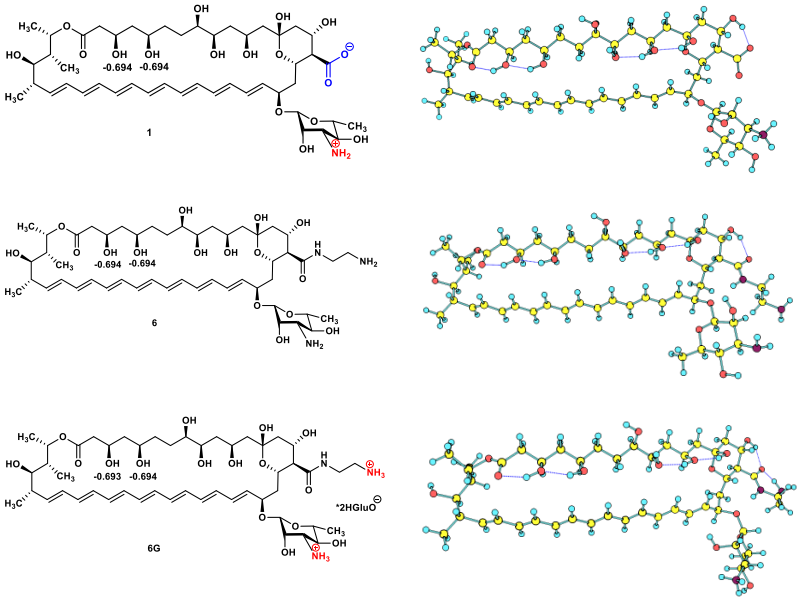

Polyene type	AmB (**1**)	**6**	**6G**
Partial charge in ligand C3-(OH) group	-0.694	-0.694	-0.693
Partial charge in ligand C5-(OH) group	-0.694	-0.694	-0.694

Figure 6. Partial charges of oxygens in ligand (OH) groups and conformations of the polyene cores of AmB (**1**), **6**, and **6G** (calculated using the density functional method B3LYP/6-31G (d).

more likely influenced by the differences in aggregation properties than by the partial charge of oxygen in the ligand C3- and C5-(OH) group.

Table 2 shows the mean dwell times, τ, and the probability of polyene channels to be open, P_{op}. The lifetime increases in the order of **6G** ≈ **6** < AmB (**1**). Moreover, P_{op} of pores induced by **6** and **6G** is two times lower than P_{op} of the channel formed by natural AmB (**1**). Taking into account that the stabilization of the AmB channel complex in an open state is due to electrostatic interactions between the ammonium and carboxyl groups of adjacent antibiotic molecules,[32] one can assume that a decrease in τ and P_{op} of pores induced by **6G** compared to AmB (**1**) is caused by electrostatic repulsion between positively charged polyene molecules, while zwitterionic parent antibiotic is more prone to aggregate. Positively charged molecules of **6G** weakly interact with each other, which promotes the destabilization of the open polyene pore. Moreover, the absence of carboxyl group may decrease the interaction between adjacent carboxamides **6** or **6G**.

Figure 6 shows the results of quantum-chemical calculations using the density functional method B3LYP/6-31G (d) of the molecular conformation of compounds **1**, **6**, and **6G** in aqueous medium. According to the NMR spectra and quantum chemical calculations, AmB molecule is a planar conformation in which a strong ionic interaction is observed between the carboxylate residue and the ammonium group of the carbohydrate moiety. In this structure, the carboxylate residue and the protons of the ammonium group of the carbohydrate fragment are spatially most close (the distance from the oxygen atom of the carboxyl group to the proton of the ammonium group is 4.7 Å) (Figure 6). It is important to note that we found that the obtained calculation results of conformation of AmB (**1**) coincided with the known data of the antibiotic conformation obtained by NMR and X-ray diffraction analysis.[35]

On the contrary, in amphamide (**6**) and its protonated form **6G**, the zwitterionic interaction is rejected, since the carboxyl group is obscured from the protons of the ammonium group of the carbohydrate fragment. A comparison of the geometry of AmB, amphamide (**6**), and its salt form **6G** shows that the comformation of the polyene core did not change significantly, while the repulsion of the positively charged amino groups in **6G** resulted in a distinct deflection of the sugar fragment from the amide residue. Taking into account that the stability of the

https://dx.doi.org/10.1021/acsinfecdis.0c00068
ACS Infect. Dis. 2020, 6, 2029−2044

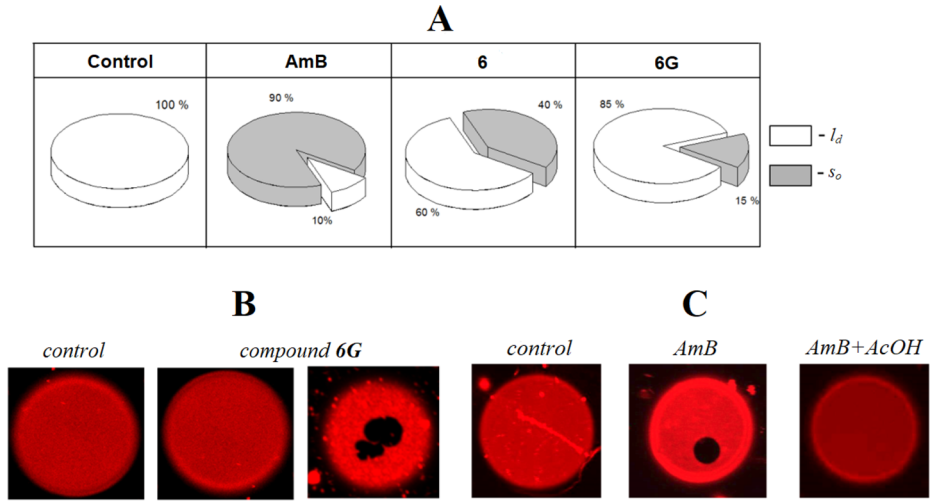

Figure 7. (A) Percentages of giant unilamellar POPC-vesicles characterized by different types of phase separation (sector related to relative number of homogeneously colored vesicles in liquid-disordered phase (l_d) is white; sector presented percentage of liposomes with gel domains (s_o) is gray) in the absence (control) and presence of 300 μM of polyenes in the liposome solution: AmB (**1**), **6**, and **6G**. (B) Fluorescence micrographs of POPC-liposomes demonstrating different types of phase separation (l_d, s_o) in the presence of 300 μM compound **6G**. (C) Fluorescence micrographs of POPC-liposomes demonstrating different types of phase separation (l_d, s_o) in the absence (control) and in the presence of 300 μM AmB or contemporaneously AmB and acetic acid (300 μM each). Size of each image is 20 × 20 μm^2.

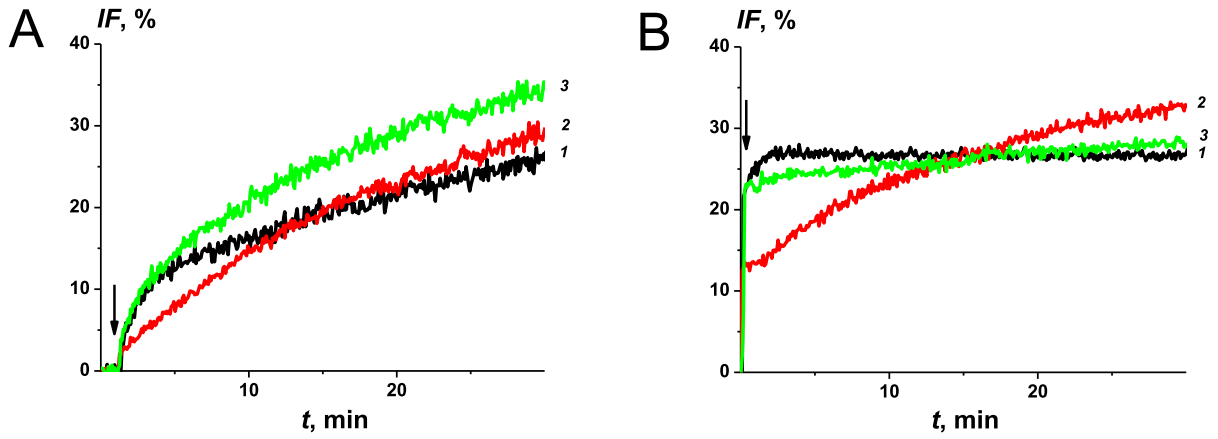

Figure 8. Dependence of relative fluorescence of calcein (*IF*, %) leaked from POPC:CHOL (67:33 mol %) (A) and POPC:ERG (67:33 mol %) (B) vesicles on time. The moment of addition of AmB (**1**), **6** (**2**), and **6G** (**3**) into liposomal suspension is indicated by an arrow. Concentration of polyene antibiotics was 50 μM.

polyene/sterol complex depends on the coplanarity of interacting molecules,[36] one can hypothesize that due to the more rigid form and parallel orientation, ERG and AmB in the AmB/ERG complex are held together by stronger van der Waals interactions than those observed between ERG and **6** or **6G** in the corresponding complex with ERG. Thus, the weakening of interactions in polyene−sterol complexes might also decrease the lifetime and the open probablity of the pores, which is observed for compounds **6** and **6G** (Table 2).

Figure 7A shows pie charts that demonstrate the percentage of phase-separated POPC-vesicles after the addition of different polyenes into a liposome suspension, P_{So}. Pure POPC liposomes do not produce uncolored gel domains at room temperature. The addition of AmB leads to phase separation in the POPC-membranes.[37,38]

Despite the observation of gel domains that exclude the fluorescent marker of the fluid disordered phase in the presence of **6**, this polyene has a lower ability to immobilize lipids than the parent antibiotic (Figure 7B). These data are in good agreement with the previous data, which demonstrated that AmB conjugates that had a modification of carboxyl group were less effective in initializing phase separation in POPC-membranes compared to the parent antibiotic.[39] The smaller P_{So}-value, which is observed (Table 2) for **6G**, may be due to the presence of the protonated form of the polyene antibiotic due to the formation of salt with L-glutamic acid. Thus, we investigated the phase segregation in POPC liposomes with the sequential addition of 300 μM AmB followed by the addition of acetic acid in with the ratio to polyene of 1:1 (mol:mol). The addition of AmB leads to the immobilization of phospholipids and the formation of gel domains, while acetic acid results in a disorder in the bilayer (Figure 7C).

Figure 8 shows the ability of AmB and compounds **6** and **6G** to disengage calcein from large unilamellar vesicles prepared from POPC and CHOL (Figure 8A) or ERG (Figure 8B) (67:33 mol %).

The first lipid mixture can be used to imitate the toxicity of polyenes toward the mammalian cells, and the second lipid

https://dx.doi.org/10.1021/acsinfecdis.0c00068
ACS Infect. Dis. 2020, 6, 2029−2044

Table 3. Characteristic Parameters of the Calcein Release from Large Unilamellar Vesicles Induced by Polyenes[a]

	POPC:CHOL (67:33 mol %)			POPC:ERG (67:33 mol %)		
Polyene	IF_{max}, %	t_1, min	t_2, min	IF_{max}, %	t_1, min	t_2, min
AmB (**1**)	23 ± 7	1.1 ± 0.4	27.4 ± 9.6	25 ± 8	0.27 ± 0.15	5.2 ± 2.7
6	29 ± 8	0.5 ± 0.2	20.2 ± 5.9	31 ± 11	0.13 ± 0.07	15.5 ± 4.4
6G	31 ± 9	0.4 ± 0.2	19.7 ± 7.9	27 ± 9	0.10 ± 0.05	20.8 ± 9.6

[a]The maximal leakage (IF_{max}) and the times related to the fast and the slow leakage component (t_1 and t_2) were obtained by fitting the time dependences of calcein leakage by two-exponential function (eq 3). The characteristic parameters of the calcein release from large unilamellar vesicles induced by 50 and 100 μM of polyene antibiotics did not differ within the measurement error, and the data were combined into one array.

Table 4. Parameters of Acute Toxicity and Antifungal Efficacy for AmB (1) and Amphamide (6G) in Mice[a]

antibiotic	MTD (mg/kg)	LD_{50} (mg/kg)	ED_{50} (mg/kg)	therapeutic index LD_{50}/ ED_{50}
AmB (**1**)	2.0 (1.73−2.14)	2.6 (2.38−2.83)	1.08	2.4
6G	9.3 (8.4−10.7)	13.8 (11.3−16.3)	0.33	41.8

[a]MTD − maximum tolerated dose (LD_{10}); LD_{50} − amount of a drug which causes the death of 50% of a group of test animals; ED_{50} − effective dose, the dose that protected 50% of the population infected by lethal dose of *C. albicans*.

mixture mimics the conditions in fungal cells. Two-exponential dependences are used to fit the time dependences of the calcein release induced by AmB and compounds **6** and **6G** from POPC:CHOL (67:33 mol %) and POPC:ERG (67:33 mol %) liposomes. The characteristic parameters of the dependences, maximal leakage (IF_{max}), and time related to fast and slow components (t_1 and t_2, respectively) are shown in Table 3.

Compounds **6** and **6G** are characterized by the slightly higher IF_{max}-value and lower t_1-value compared to those of parent antibiotic **1**. These data are in agreement with the measured threshold concentrations of antibiotics required to observe single polyene channels in CHOL- and ERG-enriched bilayers, C_{CHOL} and C_{ERG} (Table 2). Compounds **6** and **6G** are characterized by the higher ability to permeabilize ERG-containing membranes (higher IF_{max}-values and lower t_1 values) than that of the parent antibiotic, which can be the possible explanation for the threshold concentrations of AmB (**1**) required to inhibit the growth of *Candida spp.* and *A. niger* being at least 2−4-fold larger than those for **6** and **6G** (Table 1, Figure 2). Higher t_2-values observed for **6** and **6G** compared to AmB (**1**) in ERG-containing bilayers are related to the aforementioned difficulty in the aggregation of positively charged molecules of **6G** or neutral molecules of **6** as well as to the difference in the conformation of semisynthetic derivatives and the parent molecule (Figure 6), which may be important for binding with ERG.

Since the polyene induced current is proportional to the antibiotic concentration in the sixth degree,[27] the obtained 2.4-fold decrease in the threshold concentration of **6G** required to observe single polyene channels in ERG-containg bilayers compared to AmB (Table 2) corresponds to 1200-fold increase in the transmembrane current at 200 mV induced by the 1.2×10^{-7} M of **6G** relative to 1.2×10^{-7} M of AmB. The related 190-fold increase in the number of open channels and the simultaneous 2-fold decrease in P_{op} of pores (Table 2) results in 95-fold increase in NP_{op}-value which is often used to characterize the channel activity by the patch-clamp technique. This analysis clearly demonstrates the enhanced pore-forming ability of amphamide compared to natural AmB. In addition, the ratio of the threshold concentrations of polyenes in CHOL- and ERG-containing bilayers were given (Table 2). The determined C_{CHOL}/C_{ERG}-values of **6** and **6G** is higher than that of AmB (**1**), and so the toxicity of the amphamide should be lower than that for paternal AmB.

In Vivo Studies. Because the results of studies on the impact on cellular membranes showed that amphamide (**6**) had better antifungal activity and may possess a lower toxicity than those of parent AmB (**1**), the next step involved preclinical tests in mammals. Thus, the acute toxicity in mice and the antifungal efficiency of **6G** in the models of mice candidoses sepsis were evaluated and compared to those of AmB (**1**).

The acute toxicity test was performed after single intravenous administration. In general, the clinical pictures of acute toxicity and dynamics of the body weight gain/loss (data not shown) caused by the single intravenous administration of AmB or amphamide glutamate (**6G**) in mice were similar. After the administration of the highest doses, the animals in both groups died immediately after injection and exhibited the signs of neurotoxicity. Lower fatal doses led to death 2−3 min after treatment due to the same phenomena. Amphamide (**6G**) was shown to have a considerably lower acute toxicity compared to that of AmB (**1**) in these experiment; the MTD/LD_{50} values for compound **6G** and AmB were determined to be 9.3/13.6 mg/kg and 2.0/2.6 mg/kg, respectively (Table 4). Thus, the MTD value of amphamide (**6G**) was 4.6-fold higher than that of AmB, which indicated that the modification of carboxylic group of AmB lead to a considerable reduction in acute toxicity.

The tested compound **6G** demonstrated high antifungal activity in the model of mice candidosis sepsis. The study of compound **6G** and AmB in a single dose intravenous regime showed a higher efficacy of compound **6G** compared with that of AmB (ED_{50} for **6** − 0.33 mg/kg vs 1.08 mg/kg for AmB) (Tables S2 and 4). Most importantly, these in vivo antifungal activities were observed at doses corresponding to 54% of MTD for AmB and only 4% of MTD for **6**, which indicates the possibility of the much wider range of dose escalation for compound **6**. In addition, the multiple (daily four-time intravenous administration) regime demonstrated a higher antifungal efficacy of compound **6** compared with that of AmB (Table 5). The obtained results suggest that antibiotic **6G**, as well as AmB (**1**), does not accumulate in the body; its effect is limited, and multiple regimes are recommended to achieve the higher effect of the treatment.

https://dx.doi.org/10.1021/acsinfecdis.0c00068
ACS Infect. Dis. 2020, 6, 2029−2044

Table 5. Comparative In Vivo Efficacy of Amphamide (6G) and AmB (1) on a Mice Model of Candidosis Sepsis (Intravenous Four-Times Administration)

antibiotic	drug dose, mg/kg × times/period	death, %	survival, %
AmB (**1**)	0.1 × 4/24 h	60	20
	0.5 × 4/24 h	70	30
	1.0 × 4/24 h	50	50
6G	0.1 × 4/24 h	70	30
	0.5 × 4/24 h	50	50
	1.0 × 4/24 h	30	70
Control dose of *C. albicans*	3.5×10^7 CFU/mouse	100	0

Thus, the obtained results show that amphamide (**6G**) has favorable activity/toxicity properties compared to those of AmB; the therapeutic index (LD_{50}/ED_{50}) of **6G** is approximately 17-fold higher than that of paternal AmB (**1**) (41.8 vs 2.4) (Table 4).

CONCLUSION

The chemotherapy of systemic fungal infections is one of the most difficult and not yet successfully solved problems in modern medicine. This is due to the fact that both pathogenic fungi and humans are eukaryotic organisms, and it is difficult to identify an active and selective drug with low toxicity for the patient. The modification of one of the most active antifungals, amphotericin B, aiming to decrease its toxicity and increase water-solubility, has been intensively performed. However, thus far, no semisynthetic polyene antibiotics have been introduced to clinical practice.

Based on the idea of obtaining novel AmB derivatives with lower self-aggregation properties and improved antifungal efficacy, we synthesized a series of AmB amides containing basic groups in the introduced residue. The investigation of in vitro antifungal activity showed that amphamide (**6**) exhibited superior antifungal activity compared with that of AmB (**1**). The electrophysiological experiments of the selected candidate **6** suggested that it had lower self-aggregation properties but higher pore-forming abilities in the model membrane compared to those of AmB (**1**) under the same conditions.

The enhanced selectivity of amphamide (**6**) for the ERG-containing bilayers resulted in the lower toxicity of compound **6** compared to that of AmB. In vivo studies in the model of mice candidosis sepsis confirmed that compound **6** had a much lower acute toxicity and higher antifungal efficiency compared to those of AmB (**1**). Thus, a novel AmB derivative, amphamide, with a considerably increased safety and better efficacy compared to those of AmB (**1**) with a therapeutic index (LD_{50}/ED_{50}) of almost 17-fold higher than that of AmB (**1**) (42 vs 2.4) was discovered. Moreover, unlike AmB (**1**), amphamide (**6**) can be used in a water-soluble salt form (i.e., as glutamate **6G**), which considerably simplifies dosage drug formulation and application. Thus, synthesized amphamide has substantial chemotherapeutic advantages over AmB. The discovery of this drug candidate can result in the development of the second generation of polyene antibiotics for the treatment of fungal infections, which represent a growing health risk.

METHODS

General. All chemicals were purchased from commercial suppliers and used as received. Amphothericin B, PyBOP, KCl, HEPES, DMSO, KOH, and sorbitol were purchased from Sigma Chemical Corporation (St. Louis, MO, USA). Synthetic 1,2-diphytanoyl-*sn*-glycero-3-phosphocholine (DPhPC), 1-palmitoyl-2-oleoyl-*sn*-glycero-3-phosphocholine (POPC), ergosterol (ERG), cholesterol (CHOL), and 1,2-dipalmitoyl-*sn*-glycero-3-phosphoethanolamine-*N*-(lissamine rhodamine B sulfonyl) (Rh-DPPE) were obtained from Avanti Polar Lipids, Inc. (Pelham, AL). Water was distilled twice and deionized. Solutions of 2.0 M KCl were buffered using 5 mM HEPES at pH 7.0. TLC analysis was performed on the Silica gel 60 F254 plates (aluminum sheets 20 × 20 cm^2) Merck (Darmstadt, Germany) in following systems: (I) $CHCl_3$−MeOH−H_2O−HCOOH, 7:5:1.2:0.05; (II) $CHCl_3$−MeOH−H_2O−HCOOH, 13:6:0.8:0.01; (III) *n*-PrOH−EtOAc−NH_4OH, 3:3:3; (IV) *n*-PrOH−EtOAc−NH_4OH, 3:3:2; (V) $CHCl_3$−MeOH−H_2O−NH_4OH, 13:6:1:0.1. All final compounds were purified to >95% by normal phase flash or column chromatography Merck silica gel (0.040−0.063 mm) (Darmstadt, Germany), or crystallization. The purity was assessed by reverse phase HPLC which was carried out on a Shimadzu HPLC instrument of the LC 20AD series (Japan) on a Kromasil-100 C18 column (4.6 × 250 mm, particle size 5 μm, Ekzo Nobel, Sweden) with an injection volume of 20 μL (concentration of substances 0.025−0.05 mg/mL) at a flow rate of 1.0 mL/min and monitored by a diode array ultraviolet detector at 408 nm. The system consisted of buffer 0.2% $HCOONH_4$ at pH 4.5 and organic phase acetonitrile. The proportion of acetonitrile was varied from 30% to 60% for 15 min (system A), and 30% to 70% for 30 min (system B). NMR spectra were recorded on Bruker Avance III 500 MHz NMR spectrometer with 500.23 and 125.78 MHz resonance frequencies for ^1H and ^{13}C, respectively. Spectra were recorded in DMSO-d_6 solutions at 303 K and were referenced against residual solvent signals: 2.50 ppm for DMSO-d_5 for ^1H and 39.50 ppm for DMSO-d_6 for ^{13}C, respectively. Mixing times in the range of 10−180 ms were used to mimic stepwise magnetization propagation. For 2D TOCSY, a mixing time of 80 ms was used. For 2D ROESY and NOESY experiments, mixing times of 300 and 500 ms were used, respectively. Abbreviations used in describing peak signals are br = broad, s = singlet, d = doublet, dd = doublet of doublets, t = triplet, q = quartet, and m = multiplet. ESI MS spectra were recorded on a Bruker microTOF-Q II instrument (BrukerDaltonics GmbH, Bremen, Germany).

Carboxamides of Amphothericin B (2−4) (General Method A). Corresponding amine (0.44 mmol, 2 equiv of 1,4-piperazine, *N*-(2-hydroxyethyl)ethylenediamine, or 2,2′-oxidiethanamine) was added to a solution of AmB (**1**, 200 mg, 0.22 mmol) in DMSO (5 mL), then PyBOP (137 mg, 0.26 mmol) was added portionwise during 1.5 h, pH of the reaction mixture was maintained at 7−8 by an addition of Et_3N. The reaction mixture was stirred for 4 h, and then Et_2O (10 mL) was added. The mixture was stirred vigorously, and then the Et_2O layer was removed and the procedure was repeated several times until viscous oil was formed. Acetone was added to the oil; the forming precipitate was filtered off, washed with acetone, and dried in vacuum. The progress of the reactions and chromatography purification and the purity of final compounds were monitored by TLC and HPLC analysis.

https://dx.doi.org/10.1021/acsinfecdis.0c00068
ACS Infect. Dis. 2020, 6, 2029−2044

The crude amide was purified by column chromatography on silica gel.

The amide was dissolved in $CHCl_3$−MeOH mixture (2 mL) and put on a column preequilibrated with $CHCl_3$. The elution was carried out with $CHCl_3$ and then with a mixture $CHCl_3$-MeOH-H_2O-HCOOH (13:6:1:0.1). Fractions containing the target compound were combined and evaporated to a small volume. The addition of acetone to the solution gave the precipitate of formate of a targeted compound that was filtered off and dried.

*1-(Piperazin-1-yl)amide of AmB (**2**).* Yield: 41 mg (19%); yellow powder; mp. 174−176 °C (decomp.); R_f (III) 0.63; R_t (system A) 8.66 min; purity 95.3%; HRMS (ESI) *m/z*: $[M + H]^+$ Calc. for $C_{51}H_{82}N_3O_{16}$ 992.5695; Found 992.5729.

*N-(2-((2-Hydroxyethyl)amino)ethyl)amide of AmB (**3**).* Yield: 26 mg (12%); yellow powder; mp. 170−172 °C (decomp.); R_f (III) 0.60; R_t (system B) 14.65 min, purity 95.2%; HRMS (ESI) *m/z*: $[M + H]^+$ Calc. for $C_{51}H_{84}N_3O_{17}$ 1010.5801; Found 1010.5946.

*N-(2-(2-Aminoethoxy)ethyl)amide of AmB (**4**).* Yield: 55 mg (25%); yellow powder; mp. 167−169 °C (decomp.); R_f (IV) 0.38; R_t (system A) 8.74 min; purity 95.6%; HRMS (ESI) *m/z*: $[M + H]^+$ Calc. for $C_{51}H_{84}N_3O_{17}$ 1010.5801, Found 1010.5784.

*N-(2-((2-Aminoethyl)amino)ethyl)amide of AmB (**5**). I step: (9H-Fluoren-9-yl)methyl bis(2-((tert-butoxycarbonyl)-*

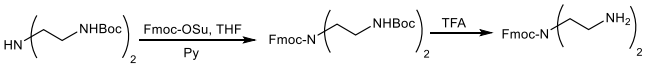

amino)ethyl)carbamate. Pyridine (0.61 mL, 7.58 mmol) was added to a stirred solution of di-*tert*-butyl(azanediylbis(ethane-2,1-diyl))dicarbamate (2.3 g, 7.58 mmol, obtained as described in ref 40) in THF (30 mL). 9-Fluorenylmethyl *N*-succinimidyl carbonate (FmocOSu, 3.8 g, 11.37 mmol) was added portionwise; the reaction mixture was stirred for 1 h at rt and then evaporated in vacuum. Ethyl acetate (30 mL) and H_2O (30 mL) were added to the residue. The organic fraction was washed with H_2O (3 × 30 mL), dried over Na_2SO_4, and concentrated in vacuum. The addition of Et_2O to the residue resulted in formation of white solid, which was filtered off and dried. The purification of the target compound was performed using column chromatography on silica gel in toluene−acetone (5:1) mixture. Fractions contained target compound were collected, and concentrated in vacuum. The addition of Et_2O to the residue resulted in formation of white solid which was filtered off and dried. Yield: 1.57 g (40%). R_f (II) 0.31.

II step: (9H-Fluoren-9-yl)methyl bis(2-aminoethyl)carbamate trifluoroacetate. Thrifluoroacetic acid (1 mL) was added to the solution of (9*H*-fluoren-9-yl)methyl bis(2-((*tert*-butoxycarbonyl)amino)ethyl)carbamate (500 mg, 0.95 mmol) in dichloromethane (10 mL). The reaction mixture was stirred for 1 h at rt and then concentrated in vacuum. The resulting viscous oil of crude (9*H*-fluoren-9-yl)methyl bis(2-aminoethyl)carbamate trifluoroacetate was used without additional purification on the next step. Yield: 1.32 g (90%). HRMS (ESI) *m/z*: $[M + H]^+$ Calc. for $C_{19}H_{24}N_3O_2$ 326.1869, Found 326.1856. ^{1}H NMR (DMSO-d_6) δ, ppm: 8.07 (6H, br. s., 2 × NH_3^+); 7.89 (2H, d, Ar-Fmoc); 7.64 (2H, d, Ar-Fmoc); 7.42 (2H, t, Ar-Fmoc); 7.35 (2H, t, Ar-Fmoc); 4.37−4.31 (3H, m, C<u>H</u>$_2$-Fmoc, C<u>H</u>-Fmoc); 3.48 (4H, m, C<u>H</u>$_2$); 2.98−2.88 (4H, m, C<u>H</u>$_2$). ^{13}C NMR (DMSO-d_6) δ, ppm: 155.8 (CO); 143.9 (CH, Ar-Fmoc); 140.7 (CH, Ar-Fmoc); 127.8 (CH, Ar-Fmoc); 127.2 (CH, Ar-Fmoc); 125.1 (CH, Ar-Fmoc); 120.2 (CH, Ar-Fmoc); 67.6 (C<u>H</u>$_2$-Fmoc); 46.6 (C<u>H</u>-Fmoc); 44.8 (C<u>H</u>$_2$); 37.4 (C<u>H</u>$_2$).

*III step: N-(2-((2-Aminoethyl)amino)ethyl)amide of AmB (**5**, Method B).* (9*H*-Fluoren-9-yl)methyl bis(2-aminoethyl)-carbamate trifluoroacetate obtained in a previous step was added to a solution of AmB (**1**, 545 mg, 0.5 mmol) in DMSO (6 mL), and then PyBOP (455 mg, 1 mmol) was added portionwise during 1.5 h; pH of the reaction mixture was maintained at 7−8 by adding Et_3N. The reaction mixture was stirred for 4 h, and then Et_2O (10 mL) was added. The mixture was stirred vigorously, and then the Et_2O layer was removed and the procedure was repeated several times until viscous oil was formed. Acetone was added to the oil; the forming precipitate was filtered off, washed with acetone, and dried in vacuum. The progress of the reactions and chromatography purification and the purity of final compounds were monitored by TLC in the system V and HPLC analysis. The crude amide was purified by column chromatography on silica gel. The amide was dissolved in $CHCl_3$−MeOH mixture (2 mL) and put on a column preequilibrated with $CHCl_3$. The elution was carried out with $CHCl_3$ (20 mL) and then with a mixture $CHCl_3$-MeOH-H_2O-HCOOH (13:6:1:0.1). Fractions containing the target compound were combined and evaporated to a small volume. The addition of acetone to the solution gave the precipitate that was filtered off and dried. The obtained amide (**Fmoc-5**, 125 mg, 0.1 mmol) was dissolved in DMSO (6 mL) and piperidine was added (40 μL, 0.41 mmol). The reaction mixture was stirred for 30 min, and then Et_2O (10 mL) was added. The mixture was stirred vigorously, and then the Et_2O layer was removed and the procedure was repeated several times until viscous oil was formed. Acetone was added to the oil; the forming precipitate was filtered off, washed with acetone, and dried in vacuum.

Yield of *N*-(2-((2-aminoethyl)amino)ethyl)amide of AmB (**5**): 98 mg (10%); yellow powder; mp. 160−163 °C (decomp.); R_f (III) 0.34; R_t (system A) 8.16 min; purity 95.0%; HRMS (ESI) *m/z*: $[M + H]^+$ Calc. for $C_{51}H_{85}N_4O_{16}$ 1009.5961, Found 1009.5849.

N-Fmoc-amphothericin B (Fmoc-1). 9-Fluorenylmethyl-*N*-succinimidyl carbonate (FmocOSu, 0.95 g, 2.8 mmol) was added portionwise to a mixture of AmB (**1**, 2.0 g, 2.2 mmol) and pyridine (0.025 mL) in the mixture DMF−MeOH (20 mL, 5:1). The mixture was stirred for 5 h and was poured into an excess of Et_2O. The residue was filtered, washed by Et_2O, and dried in vacuo. The obtained crude N-Fmoc AmB (purity 81% by HPLC) was purified by column chromatography on silica gel ($CHCl_3$-MeOH-H_2O-NH_4OH, 13:6:1:0.1) to yield 2.16 g (88%) of *N*-Fmoc-AmB (**Fmoc-1**) of 95% purity. HRMS (ESI) *m/z*: $[M + H]^+$ Calc. for $C_{62}H_{83}NO_{19}$ 1146.5638, Found 1146.5917. ^{1}H NMR (DMSO-d_6) δ, ppm: 8.20−7.33 (8H, m, Fmoc); 7.01 (1H, m, 3′-NH); 6.43 (1H, m, 24-CH); 6.38 (1H, m, 22-CH); 6.32 (1H, m, 26-CH); 6.29 (1H, m, 29-CH); 6.29 (1H, m, 30-CH); 6.28 (1H, m, 25-CH); 6.25 (1H, m, 23-CH); 6.16 (1H, m, 31-CH); 6.15 (1H, m, 27-CH); 6.08 (1H, m, 21-CH); 6.07 (1H, m, 32-CH); 5.96 (1H, m, 20-CH); 5.43 (1H, m, 33-CH); 5.20 (1H, m, 37-CH); 5.0 (2H, m, CH_2-Fmoc); 4.66 (1H, m, CH-Fmoc); 4.47 (1H, m, 1′-CH); 4.37 (1H, m, 19-CH); 4.22 (1H, m, 11-CH); 4.19 (1H, m, 17-CH); 4.05 (1H, m, 3-CH); 3.96 (1H, m, 15-CH); 3.66 (1H, m, 2′-CH); 3.52 (1H, m, 5-CH); 3.45 (1H, m, 9-CH); 3.42 (1H, m, 3′-CH); 3.17 (1H, m, 4′-CH); 3.17 (1H, m, 5′-CH); 3.09 (1H, m, 35-CH); 3.08 (1H, m, 8-CH); 2.28

https://dx.doi.org/10.1021/acsinfecdis.0c00068
ACS Infect. Dis. 2020, 6, 2029−2044

(1H, m, 34-CH); 2.16 (2H, m, 2-CH_2); 2.06 (2H, m, 18-CH_2); 1.9 (1H, m, 16-CH); 1.86 (2H, m, 14-CH_2); 1.72 (1H, m, 36-CH); 1.57 (1H, m, 7-CH); 1.57 (1H, m, 18-CH); 1.55 (1H, m, 10-CH); 1.53 (2H, m, 12-CH_2); 1.39 (1H, m, 6-CH);1.39 (1H, m, 4-CH); 1.31 (1H, m, 4-CH); 1.30 (1H, m, 10-CH); 1.25 (1H, m, 6-CH); 1.24 (1H, m, 7-CH); 1.16 (3H, m, 6′-CH_3); 1.11 (3H, m, 37-CH_3); 1.09 (1H, m, 14-CH); 1.03 (3H, m, 34-CH_3); 0.91 (3H, m, 36-CH_3). ^{13}C NMR (DMSO-d_6) δ: 136.6 (C20); 136.5 (C33); 133.7 (C24); 133.4 (C26); 133.3 (C22); 132.9 (C30); 132.0 (C29); 131.9 (C27); 131.9 (C25); 131.6 (C23); 131.6 (C31); 131.0 (C32); 128.4 (C21); 96.7 (C1′); 76.9 (C8); 74.5 (19); 73.5 (C9); 73.3 (C35); 73.0 (C5′); 69.4 (C4′); 69.0 (5); 68.8 (C2′); 68.6 (C37); 66.0 (C3); 65.4 (C11); 65.2 (C15); 65.1 (C17); 56.7 (C3′); 56.5 (C16); 46.0 (C12); 44.5 (C4); 44.1 (C14); 42.2 (C34); 41.8 (C2); 39.4 (C36); 39.3 (C10); 37.0 (C18); 35.9 (C6); 28.8 (C7); 18.2 (34Me); 17.9 (C6′); 16.7 (C37Me); 11.8 (C36Me).

*Carboxamides of Amphothericin B (**6**−**10**) (General Method C).* Corresponding amine (1,2-diaminoethane, 1,3-diaminopropane, 1-(2-aminoethyl)guanidine, 3-(aminomethyl)pyridine, or 4-(aminomethyl)pyridine) (0.14 mmol) was added to a solution of *N*-Fmoc-AmB (**Fmoc-1**, 80 mg, 0.07 mmol) in DMSO (5 mL), and then PyBOP (55 mg, 0.105 mmol) was added portionwise during 1.5 h; pH of the reaction mixture was maintained at 7−8 by adding Et_3N. The reaction mixture was stirred for 4 h, and then Et_2O (10 mL) was added. The mixture was stirred vigorously, and then the Et_2O layer was removed and the procedure was repeated several times until viscous oil was formed. Acetone was added to the oil; the forming precipitate was filtered off, washed with acetone, and dried in vacuum. The crude amide was purified by column chromatography on silica gel. The *N*-Fmoc-protected amide was dissolved in $CHCl_3$−MeOH mixture (2 mL) and put on a column preequilibrated with $CHCl_3$. The elution was carried out with $CHCl_3$ (20 mL) and then with a mixture $CHCl_3$-MeOH-H_2O-HCOOH (13:6:1:0.1). Fractions containing a *N*-Fmoc-derivative of the target compound were combined and evaporated to a small volume. The addition of acetone to the solution gave the precipitate that was filtered off and dried. The obtained amide was dissolved in DMSO (6 mL) and piperidine was added (100, 1.0 mmol). The reaction mixture was stirred for 30 min, and then Et_2O (10 mL) was added. The mixture was stirred vigorously, and then the Et_2O layer was removed and the procedure was repeated several times until viscous oil was formed. Acetone was added to the oil; the forming precipitate of the target compound was filtered off, washed with acetone, and dried in vacuum.

*N-(2-Aminoethyl)amide of AmB (**6**).* Yield: 28 mg (41% from *N*-Fmoc-AmB (**7**)); yellow powder; mp. 115−118 °C (decomp.); R_f (IV) 0.42; R_t (system A) 8.57 min; purity 95.9%; HRMS (ESI) *m*/*z*: $[M + H]^+$ Calc. for $C_{49}H_{80}N_3O_{16}$ 966.5539, Found 966.5775. ^{1}H NMR (DMSO-d_6) δ, ppm: 8.34 (1H, m, NH); 6.45 (1H, m, 24-CH); 6.38 (1H, m, 22-CH); 6.35 (1H, m, 28-CH); 6.31 (2H, m, 25-CH; 26-CH); 6.28 (2H, m, 27-CH; 29-CH); 6.25 (1H, m, 23-CH); 6.16 (1H, m, 31-CH); 6.15 (1H, m, 30-CH); 6.10 (1H, m, 21-CH); 6.07 (1H, m, 32-CH); 5.93 (1H, dd, *J* = 15.1, *J* = 9.1; 20-CH); 5.44 (1H, dd, *J* = 14.9, *J* = 10.0; 33-CH); 5.20 (1H, bq, *J* = 6.7, 37-CH); 4.35 (1H, m, 19-CH); 4.33 (1H, m, 1′-CH); 4.24 (1H, m, 11-CH); 4.23 (1H, m, 17-CH); 4.06 (1H, m, 3-CH); 4.02 (1H, m, 15-CH); 3.73 (1H, m, 2′-CH); 3.54 (1H, t, *J* = 9.1, 5-CH); 3.46 (1H, bd, *J* = 10.0, 9-CH); 3.25 (2H, m, 1″-CH_2); 3.11 (1H, m, 8-CH); 3.10 (1H, m, 5′-CH); 3.07 (1H, m, 4′-CH); 2.75 (2H, m, 2″-CH_2); 2.67 (1H, m, 3′-CH); 3.09 (1H, m, 35-CH); 2.28 (1H, m, 34-CH); 2.18 (2H, m, 2-CH_2); 1.94 (1H, m, 18-CH); 1.94 (1H, m, 16-CH); 1.88 (1H, m, 14-CH); 1.73 (1H, m, 36-CH); 1.57 (1H, m, 7-CH); 1.55 (1H, m, 10-CH); 1.53 (2H, m, 12-CH_2); 1.46 (1H, m, 18-CH); 1.40 (1H, m, 4-CH); 1.39 (1H, m, 6-CH); 1.35 (1H, m, 4-CH); 1.32 (1H, m, 10-CH); 1.29 (1H, m, 6-CH); 1.27 (1H, m, 7-CH); 1.15 (3H, d, *J* = 5.3, 6′-CH_3); 1.11 (3H, d, *J* = 6.7, 37-CH_3); 1.09 (1H, m, 14-CH); 1.04 (3H, d, *J* = 6.3, 34-CH_3); 0.92 (3H, d, *J* = 7.1, 36-CH_3). ^{13}C NMR (DMSO-d_6) δ:172.5 (C═O); 170.6 (C1); 136.7 (C33); 136.5 (C20); 133.8 (C24); 133.6 (C28); 133.4 (C22); 133.1 (C26); 132.3 (C29); 132.3 (C25); 132.2 (C27); 132.1 (C31); 131.8 (C23); 131.8 (C30); 131.1 (C32); 128.8 (C21); 97.1 (C13); 96.7 (C1′); 77.1 (C35); 74.7 (C19); 73.7 (C9); 73.6 (C8); 73.0 (C5′); 71.0 (C4′); 69.2 (C5); 68.9 (C37); 68.4 (C2′); 67.7 (C11); 66.2 (C3); 64.8 (C15); 65.2 (C17); 57.1 (C16); 56.0 (C3′); 46.3 (C12); 44.7 (C4); 44.5 (C14); 42.3 (C34); 42.1 (C2); 39.7 (C36); 39.6 (C10); 39.4 (C2″); 38.5 (C1″); 36.7 (C18); 35.0 (C6); 29.0 (C7); 18.5 (34Me); 17.8 (C6′); 16.9 (C37Me); 12.0 (C36Me).

*L-Glutamate of N-(2-Aminoethyl)amide of AmB (**6G**).* *N*-(2-Aminoethyl)amide of AmB (**6**, 100 mg, 0.1 mmol) was added to a stirred solution of L-glutamic acid (30 mg, 0.2 mmol) in H_2O (10 mL); the mixture was stirred for 15 min, filtered, frizzed at −18 °C for 5 h, and lyophilized in vacuum. Yield: 130 mg (100%), light yellow powder. R_t (system A) 8.63 min; purity 95.5%. mp. 160−163 °C (decomp.).

*N-(2-Aminopropyl)amide of AmB (**7**).* Yield: 14 mg (21% from *N*-Fmoc-AmB (**7**)); yellow powder; mp. 165−167 °C (decomp.); R_f (IV) 0.31; R_t (system A) 7.44 min; purity 95.2%; HRMS (ESI) *m*/*z*: $[M + H]^+$ Calc. for $C_{50}H_{82}N_3O_{16}$ 980.5695, Found 980.5701.

*N-(2-Guanidinoethyl)amide of AmB (**8**).* *I step: N-Boc-ethylenediamine hydrochloride.* Solution of ammonium chloride (340 mg, 6.3 mmol) in H_2O (5 mL) was added to the solution of *N*-Boc-ethylenediamine (1.0 g, 6.3 mmol) in MeOH (3.5 mL). The mixture was stirred for 15 min and evaporated in vacuum to dryness. Yield: 1.2 g (97%) as white solid.

II step: 1-(2-aminoethyl)guanidine dihydrochloride. 1-*H*-Pyrazol-1-carboaximidine hydrochloride (745 mg, 5.1 mmol) and *N*,*N*-diisopropylethylamine (1.77 mL) were added to a stirred solution of *N*-Boc-ethylenediamine hydrochloride (1.0 g, 5.1 mmol) in DMF (25 mL). The reaction mixture was stirred at 60 °C for 2 h, cooled to rt, and Et_2O (20 mL) was added. The mixture was stirred vigorously, and then the Et_2O layer was removed and the procedure was repeated several times until viscous oil was formed. The oil residue was dissolved THF (15 mL), and 3 N HCl in Et_2O (5 mL) was added. The mixture was stirred at rt for 1 h; the forming precipitate was filtered off and dried to give 1-(2-aminoethyl)-guanidine dihydrochloride (660 mg, yield 94%). The characteristics of the obtained compound fully corresponded to those earlier described.[41]

*III step: N-(2-Guanidinoethyl)amide of AmB (**8**).* Derivative **8** was obtained from *N*-Fmoc-AmB (**Fmoc-1**) and 1-(2-aminoethyl)guanidine dihydrochloride by general method C. Yield: 19 mg (27% from *N*-Fmoc-AmB (**Fmoc-1**)); yellow powder; mp. 155−157 °C (decomp.); R_f (III) 0.57; R_t (system A) 8.96 min; purity 95.5%; HRMS (ESI) *m*/*z*: $[M + H]^+$ Calc. for $C_{50}H_{82}N_5O_{16}$ 1008.5757, Found 1008.5754.

https://dx.doi.org/10.1021/acsinfecdis.0c00068
ACS Infect. Dis. 2020, 6, 2029−2044

*N-(Pyridin-3ylmethyl)amide of AmB (**9**).* Yield: 17 mg (24% from *N*-Fmoc-AmB (**Fmoc-1**)); yellow powder; mp. 160−162 °C (decomp.); R_f (IV) 0.46; R_t (system B) 14.01 min; purity 95.2%; HRMS (ESI) *m/z*: $[M + H]^+$ Calc. for $C_{53}H_{80}N_3O_{16}$ 1014.5539, Found 1014.5548.

*N-(Pyridin-4ylmethyl)amide of AmB (**10**).* Yield: 24 mg (34% from *N*-Fmoc-AmB (**Fmoc-1**)); yellow powder; mp. 158−160 °C (decomp.); R_f (IV) 0.46; R_t (system B) 13.62 min; purity 95.1%; HRMS (ESI) *m/z*: $[M + H]^+$ Calc. for $C_{53}H_{80}N_3O_{16}$ 1014.5539, Found 1014.5548.

In Vitro Antifungal Assay. Organisms. Strains of *Candida spp*. and dermatophytes used in this study were obtained from Medical Microbiology Laboratory of State Research Center for Antibiotics (Moscow, Russia). Strains of *Candida spp*. and spores of filamentous fungus were stored in medium supplemented with 10% (vol/vol) glycerol at −80 °C. Reference strain *C. parapsilopsis* ATCC 22019 was used as control in each experiment.

Preparation of the Samples. All of the test compounds were dissolved to prepare stock concentration of 10 mg/mL in DMSO (Merck, Darmstad, Germany). The dissolved stock solutions were then diluted in the assay nutrient medium RPMI1640 (Merck) to obtained initial concentration of 64 μg/mL and then were serially diluted for the testing of MIC. The final range of concentrations of was 0.015−32 μg/mL.

Antifungal Activity Testing. Antifungal activity testing was performed by the CLSI broth microdilution methods according to the Clinical and Laboratory Standards Institute (CLSI) M27-A3 and M38-A methods. Twenty-four-hour-old culture of *Candida spp*. and about 3 week culture of dermatophyte were grown in Sabouraud dextrose agar and used to evaluate sensitivity to antimicrobial agents.

For inoculum preparation of dermatophyte, part of the colony was transferred to sterile distilled water containing 0.1% Tween 80, and shaken vigorously. The suspension was filtered through sterile gauze, and the number of spores and conidia were counted using a hemocytometer, and used as a stock spore solution for inoculum. Final inoculum suspensions were adjusted to 10^4 spores and conidia/mL. The colonies of yeast cells were suspended in sterile saline and adjusted to give a final concentration of 10^3 cells/mL.

Minimum inhibitory concentration (MIC) was defined as the lowest concentration that gave complete growth inhibition after incubation for 24 and 48 h for *Candida spp* and 48−72 h for dermatophytes.

UV Spectrophotometry. Dimerization of the amphamide (**6G**) and AmB was determined using the absorption spectra. UV absorption spectra for AmB and compound **6G** were obtained in the following manner. Aliquots of the polyene (stock solution in DMSO for AmB and in PBS for **6G** were added to Dulbecco's PBS solution at pH = 7.46 at different concentrations and used to obtain the absorption spectra in a UV/vis double beam spectrometer (UV-2804, UNICO, Dayton, NJ, USA) at rt.

Model Membrane Experiments. Registration of Ion Channels in Planar Lipid Bilayers. Virtually solvent-free planar lipid bilayers were prepared according to a monolayer-opposition technique[42] on a 50-μm-diameter aperture in a 10-μm-thick Teflon film separating two (*cis* and *trans*) compartments of the Teflon chamber. The aperture was pretreated with hexadecane. The lipid bilayers were made from 67 mol % DPhPC and 33 mol % ERG (or CHOL) using 1−2 mg/mL stock lipid solution in pentane. Model lipid membranes were bathed in 2.0 M KCl (5 mM HEPES, pH 7.4). After the membrane was completely formed and stabilized, electrical stability was assessed by applying voltages in the range from −200 to 200 mV with 50 mV step for 5−10 min. Polyene antibiotics (AmB (**1**) or compound **6** and **6G**) from a stock solution (1 mM in DMSO for AmB and **6**, and in H_2O for **6G**) were initially added to cis-compartment of Teflon chamber up to 0.2×10^{-7} M. If channel-like activity had not been observed for 15−20 min, another 0.1×10^{-7} M of antibiotic was added at the *cis*-side of the membrane, and so forth. This process was repeated until single channel activity was observed. For **1**, **6**, and **6G** single channel formation was observed at various concentrations that mean value presented in the Table 2. The polyene concentration depended on membrane sterol composition and antibiotic type varied in the range from 0.3×10^{-7} to 2.7×10^{-7} M that corresponded to the lipid:polyene molar ratio from 70:1 to 8:1. Ag/AgCl electrodes with agarose/2 M KCl bridges were used to apply a transmembrane voltage (V) and measure the transmembrane current (I). "Positive voltage" refers to the case in which the *cis*-side compartment was positive with respect to the *trans*-side. All experiments were performed at room temperature. The final concentration of solvent in the chamber did not exceed 10^{-4} mg/mL and did not produce any changes in the stability and conductance of the bilayers.

Current measurements were performed using an Axopatch 200B amplifier (Molecular Devices, LLC, Orlean, CA, USA) in the voltage clamp mode. Data were digitized by a Digidata 1440A and analyzed using a pClamp 10 (Molecular Devices, LLC, Orlean, CA, USA) and Origin 7.0 (OriginLab Corporation, Northampton, MA, USA). Current tracks were filtered by an 8-pole Bessel 100 kHz. Single-channel conductance (G) was defined as the ratio between the current flowing through a single polyene channel (I) and transmembrane potential (V). The total numbers of events used for the channel conductance fluctuation and dwell time analysis were 500−1000 and 1500−2000, respectively. The time (τ) and probability (P_{op}) of the polyene channels to be in an open state were determined using pClamp 10. The parameters of single polyene channels (G, τ, and P_{op}) were measured at V equal to 50, 100, 150, and 200 mV.

Confocal Fluorescence Microscopy of Giant Unilamellar Vesicles. Giant unilamellar vesicles were formed by the electroformation method on a pair of indium tin oxide (ITO) slides using a commercial Nanion vesicle prep pro (Munich, Germany) as previously described.[37,43] Lipid stock solutions of POPC were prepared in chloroform. Labeling was achieved by addition of the fluorescent lipid probe Rh-DPPE; its concentration in each sample was 1 mol %. The resulting aqueous liposome suspension containing 1 mM lipid and 0.5 M sorbitol was divided into 50 mL aliquots. Polyenes were added into aliquots to a final concentration of 300 μM that corresponded to the lipid:polyene molar ratio of 3.3:1. The liposome suspension with polyenes was allowed to equilibrate for 30 min at room temperature (25 ± 1 °C). The sample was observed as a standard microscopy preparation, and 10 μL of the resulting liposome suspension without and with polyenes was placed on a standard microscope slide and covered by a coverslip. Vesicles were imaged through an oil immersion objective (65×/1.4HCX PL) using a Olympus (Germany). The temperature during observation was controlled by air heating/cooling in a thermally insulated camera.

https://dx.doi.org/10.1021/acsinfecdis.0c00068
ACS Infect. Dis. 2020, 6, 2029−2044

Rh-DPPE clearly favors a liquid disordered phase (l_d) and is excluded from the gel (s_o) phase.[44] The percentage of vesicles with gel domains (P_{So}) was calculated as the ratio of phase-separated liposomes (N_{So}) to the total number of analyzed GUVs (N_t)

$$P_{So} = \frac{N_{So}}{N_t} \cdot 100\% \quad (1)$$

At least 3−5 independent experiments were performed with each combination of tested polyene and sterol; the total number of counted vesicles in the sample was typically equal to 50.

Calcein Release from Large Unilamellar Vesicles. The fluorescence of calcein leaked from large unilamellar vesicles was used to monitor the membrane permeabilization induced by AmB (**1**) and compounds **6** and **6G**. LUVs were prepared from POPC:CHOL (67:33 mol %) and POPC:ERG (67:33 mol %) by extrusion using an Avanti Polar Lipid mini-extruder (Pelham, AL) as described early.[27] Polyenes from stock solution were added to calcein-loaded liposomes. Time-dependent on calcein fluorescence dequenching induced by 50−100 μM of polyenes had been measured during 30 min. The antibiotic concentrations of 50 μM and 100 μM corresponded to the lipid:polyene molar ratios of 20:1 and 10:1, respectively.

The degree of calcein release was determined at 25 °C using spectrofluorimeter "Fluorat-02-Panorama" production "Lumex" (Saint-Petersburg, Russia). The excitation wavelength was 490 nm and the emission wavelength was 520 nm. Addition of Triton X-100 from 10 mM water solution to a final concentration of 0.1 M to each sample led to complete disruption of vesicles, and the intensity of fluorescence after releasing the total amount of calcein from liposomes was measured.

The relative intensity of calcein fluorescence (*IF*, %) was used to describe the dependence of the permeabilization of the liposomes on the type of the membrane active compound. *IF* was calculated using the following formula

$$IF = \frac{I - I_0}{I_{max}/0.9 - I_0} \cdot 100\% \quad (2)$$

where I and I_0 were the calcein fluorescence intensities in the sample in the presence and in the absence of polyenes, respectively, and I_{max} was the maximal fluorescence of the sample after lysis of liposomes by Triton X-100. A factor of 0.9 was introduced to calculate the dilution of the sample by Triton X-100.

Time dependences of leakage $IF(t)$ were fitted with two-exponential functions with characteristics times t_1 and t_2 related to fast and slow components of calcein release

$$IF(t) = A_1 \cdot \exp\left(-\frac{t}{t_1}\right) + A_2 \cdot \exp\left(-\frac{t}{t_2}\right) + IF_{max} \quad (3)$$

where IF_{max} is the maximal marker leakage, A_1 and A_2 are arbitrary constants that weigh the fast and slow time constants t_1 and t_2, respectively.

Quantum Chemical Calculations. The calculations were carried out using the density functional method B3LYP/6-31G (d)[34] using the Gaussian 09 software package[45] with full optimization of geometric parameters. To optimize the geometry of the molecules under study, we used solvent modeling (water) according to the standard SCRF (Self Consistent Reaction Field) procedure using the PCM (Polarizable Continuum Model) method of the Gaussian 09 program.[45] The affiliation of the calculated structures to the regions of the minimum PES is proved by the calculation of vibrational structures, the calculated values of which have only positive values.

Ethics Statement on Animal Studies. The animal study was performed in accordance with the European Convention for the Protection of Vertebrate Animals, Directives 86/609/EEC,[46] European Convention for the humane methods for the animal welfare and maintenance,[47] and the National Standard of the Russian Federation R 53434-2009 "Good Laboratory Practice",[48] and approved by Ethics of Animal Experimentation of Gause Institute of New Antibiotics.

In Vivo Testing of Acute Toxicity. The study was performed using adult SHK mice obtained from the animal breeding unit of the Russian Academy of Sciences. The animals were caged in groups of six and acclimatized for 2 weeks. They were maintained under standard laboratory conditions and had free access to standard laboratory food and water throughout the experiment. The SHK mice (20−22 g) were randomized into groups (n = 6) and received AmB (**1**) or compound **6G** as single intravenous injections. AmB (5.0 mg) was mixed with dry sodium deoxycholate (4.1 mg) in a sterile glass vial; 10 mL of phosphate buffer (NaH_2PO_4, 1.59 g; Na_2HPO_4, 0.96 g; and H_2O, to 100 mL) was added and immediately subjected to vigorous shaking for 10 min until homogeneous suspension was formed. The obtained suspension was placed into the new sterile glass vials, 5% neutral sterile glucose solution was added, and the resulting solutions (0.08% concentration) were used for intravenous administration. Compound **6G** was dissolved in 5% glucose solution to the concentration 0.05%.

Freshly prepared antibiotic solutions were individually injected into the mouse's tail vein at <0.5 mL per minute. Each antibiotic was used in a range of doses resulting in 0% to 100% lethality and a minimum of three intermediate doses.

Acute toxicity was estimated by mortality and survival time, as well as by the dynamics of the body weight gain/loss, food consumption, and clinical picture of intoxication including behavioral reactions. Animals were observed for 30 days after the last death case, and then the surviving animals were euthanized and subjected to necropsy for examination of internal abnormalities. The LD_{50} values and the maximum tolerated doses (MTD = LD_{10}) were calculated by the method of Litchfield and Wilcoxon using the StatPlus 2006 AnalystSoft StatPlus software.

Study of the Antifungal Efficiency on a Model of Mice Candidosis Sepsis. The antifungal efficiency of compound **6G** in comparison with AmB was determined on model of mice candidosis sepsis. The study was performed using adult male SHK mice (weight 18−20 g) obtained from the animal breeding unit of the Russian Academy of Sciences. Animals were maintained in plastic cages (with hardwood bedding in environmentally controlled room: 24 ± 1 °C, 12/12 h light/dark cycle) on a standard diet of bricketed forages with an easy approach to drinking water (ad libitum). After 2 week quarantine, healthy animals were randomized into groups (10 animals in a group) and used in experimental work. *C. albicans* (strain ATCC14053) was used as the infectious agent.

As a first step 100% lethal dose (LD_{100}) for *C. albicans* was determined. To this end, a suspension of the daily culture of *C. albicans* was diluted to 2×10^7, 2.5×10^7, 3.0×10^7, 3.5×10^7, and 4.0×10^7 CFU/mouse and administrated intravenously to

https://dx.doi.org/10.1021/acsinfecdis.0c00068
ACS Infect. Dis. 2020, 6, 2029−2044

mice as a single dose. The observation period was 14 days. The minimum infecting dose of *C. albicans* which caused 100% death of mice (LD_{100}) was 3.5×10^7 CFU/mouse.

Solutions of the tested drugs (compound **6G** or AmB) were prepared *ex tempore* as described above. Animals were infected with *C. albicans* (3.5×10^7 CFU/mouse) and the solutions of the tested drugs were administrated intravenously 1 h after administration of the infecting agent in the dose range from 0.1 mg/kg to 2.5 mg/kg for the single dose regime, and from 0.1 mg/kg to 1.0 mg/kg when administered four times (multiple regime, 4 times, daily administration).

The observation period was 40 days. During this period, the number of dead animals and the period of their death were recorded daily; live animals were examined daily and their body weight was determined three times a week. On day 40, the surviving mice were weighed and euthanized. To evaluate the effectiveness of the tested drugs, an indicator of 50% of the effective dose, ED_{50}, determined according to the Behrens method (frequency accumulation method), was used.

■ ASSOCIATED CONTENT

Supporting Information

The Supporting Information is available free of charge at https://pubs.acs.org/doi/10.1021/acsinfecdis.0c00068.

Table S1: ^1H and ^{13}C spectra assignment for compounds **2**−**10**; Figures S1−S18: NMR spectra for compounds **2**−**10**; Figures S22−S31: HPLC analysis for compounds **2**−**10**; Table S2: Comparative in vivo efficacy of compound **6G** and AmB (**1**) on a mice model of candidosis sepsis (intravenous single administration) (PDF)

■ AUTHOR INFORMATION

Corresponding Author

Anna N. Tevyashova − *Gause Institute of New Antibiotics, Moscow 199021, Russia; D. Mendeleev University of Chemical Technology of Russia, Moscow 125047, Russia;* orcid.org/0000-0003-1091-1011; Phone: +7-499-246-06-36; Email: chulis@mail.ru

Authors

Elena N. Bychkova − *Gause Institute of New Antibiotics, Moscow 199021, Russia*

Svetlana E. Solovieva − *Gause Institute of New Antibiotics, Moscow 199021, Russia*

George V. Zatonsky − *Gause Institute of New Antibiotics, Moscow 199021, Russia*

Natalia E. Grammatikova − *Gause Institute of New Antibiotics, Moscow 199021, Russia*

Elena B. Isakova − *Gause Institute of New Antibiotics, Moscow 199021, Russia*

Elena P. Mirchink − *Gause Institute of New Antibiotics, Moscow 199021, Russia*

Ivan D. Treshchalin − *Gause Institute of New Antibiotics, Moscow 199021, Russia*

Eleonora R. Pereverzeva − *Gause Institute of New Antibiotics, Moscow 199021, Russia*

Evgeny E. Bykov − *Gause Institute of New Antibiotics, Moscow 199021, Russia*

Svetlana S. Efimova − *Institute of Cytology of the Russian Academy of Sciences, St. Petersburg 194064, Russia*

Olga S. Ostroumova − *Institute of Cytology of the Russian Academy of Sciences, St. Petersburg 194064, Russia*

Andrey E. Shchekotikhin − *Gause Institute of New Antibiotics, Moscow 199021, Russia; D. Mendeleev University of Chemical Technology of Russia, Moscow 125047, Russia*

Complete contact information is available at: https://pubs.acs.org/10.1021/acsinfecdis.0c00068

Author Contributions

A.N.T., A.E.S. wrote the manuscript and contributed to the design and execution of the project. A.N.T., E.N.B., A.E.S. designed, coordinated, and performed synthesis of the compounds. G.V.Z. carried out the HNR studies. N.E.G. performed investigation of the in vitro antifungal activity of the synthesized compounds. S.E.S. conducted HPLC analysis. I.D.T., E.R.P., E.P.M., E.B.I designed, coordinated, and interpreted *in vivo* studies. E.E.B. carried out and interpreted quantum chemical calculations. S.S.E. and O.S.O. designed, coordinated, and interpreted model membrane experiments.

Notes

The authors declare no competing financial interest.

■ ACKNOWLEDGMENTS

Study of chemical modification of AmB was funded by RFBR, project number 20-04-00467. Electrophysiological experiments were funded by the Grant of President of the Russian Federation (#MD-2711.2019.4). Preclinical study of amphamide were supported by the State Contract with Ministry of Science and Higher Education of the Russian Federation No. 14N08.11.0193.

■ ABBREVIATIONS

AIDS, acquired immune deficiency syndrome; AmB, amphothericin B; Boc, *tert*-butoxycarbonyl; br, broad; CFU, colony-forming unit; CHOL, cholesterol; d, doublet; dd, doublet of doublets; DMF, dimethylformamide; DMSO, dimethyl sulfoxide; DPhPC, 1,2-diphytanoyl-*sn*-glycero-3-phosphocholine; ED_{50}, 50% effective dose, the dose that produces an effect in 50% of the population; ERG, ergosterol; equiv, equivalent; Et, ethyl; Fmoc, 9-fluorenylmethoxycarbonyl; Fmoc-OSu, 9-Fmoc-*N*-oxysuccinimide ester; GUV, giant unilamellar vesicles; HEPES, 4-(2-hydroxyethyl)-1-piperazineethanesulfonic acid; HR-ESI, high-resolution electrospray ionization; ITO, indium tin oxide; LD, lethal dose; m, multiplet; MIC, minimum inhibitory concentration; MTD (LD_{10}), maximum tolerated dose; POPC, 1-palmitoyl-2-oleoyl-*sn*-glycero-3-phosphocholine; Py, pyridine; PyBOP, benzotriazol-1-yl-oxytripyrrolidinophosphonium hexafluorophosphate; q, quartet; Rh-DPPE, 1,2-dipalmitoyl-*sn*-glycero-3-phosphoethanolamine-*N*-(lissamine rhodamine B sulfonyl); s, singlet; THF, tetrahydrofuran; t, triplet

■ REFERENCES

(1) Tudela, J. L. R., and Denning, D. W. (2017) Recovery from serious fungal infections should be realisable for everyone. *Lancet Infect. Dis. 17*, 1111−1113.

(2) Brown, G. D., Denning, D. W., Gow, N. A., Levitz, S. M., Netea, M. G., and White, T. C. (2012) Hidden killers: human fungal infections. *Sci. Transl. Med. 4*, 165rv13.

(3) Hamill, R. J. (2013) Amphotericin B formulations: a comparative review of efficacy and toxicity. *Drugs 73*, 919−934.

(4) Omelchuk, O. A., Tevyashova, A. N., and Shchekotikhin, A. E. (2018) Recent advances in antifungal drug discovery based on polyene macrolide antibiotics. *Russ. Chem. Rev. 87*, 1206−225.
(5) Bolard, J. (1986) (1986) How do polyene macrolide antibiotics affect the cellular membrane properties? *Biochim. Biophys. Acta, Rev. Biomembr. 864*, 257−04.
(6) de Kruijff, B., and Demel, R. A. (1974) Polyene antibiotic-sterol interactions in membranes of *Acholeplasma laidlawii* cells and lecithin liposomes. III. Molecular structure of the polyene antibiotic-cholesterol complexes. *Biochim. Biophys. Acta, Biomembr. 339*, 57−70.
(7) Andreoli, T. E. (1974) The structure and function of AmB-cholesterol pores in lipid bilayer membranes. *Ann. N. Y. Acad. Sci. 235*, 448−468.
(8) Cotero, B. V., Rebolledo-Antúnez, S., and Ortega-Blake, I. (1998) On the role of sterol in the formation of the amphotericin B channel. *Biochim. Biophys. Acta, Biomembr. 1375*, 43−51.
(9) Haido, R. M., and Barreto-Bergter, E. (1989) Amphotericin B-induced damage of *Trypanosoma cruzi* epimastigotes. *Chem.-Biol. Interact. 71*, 91−103.
(10) Sangalli-Leite, F., Scorzoni, L., Mesa-Arango, A. C., Casas, C., Herrero, E., Gianinni, M. J., Rodriguez-Tudela, J. L., Cuenca-Estrella, M., and Zaragoza, O. (2011) Amphotericin B mediates killing in *Cryptococcus neoformans* through the induction of a strong oxidative burst. *Microbes Infect. 13*, 457−467.
(11) Gray, K. C., Palacios, D. S., Dailey, I., Endo, M., Uno, B. E., Wilcock, B. C., and Burke, M. D. (2012) Amphotericin primarily kills yeast by simply binding ergosterol. *Proc. Natl. Acad. Sci. U. S. A. 109*, 2234−2239.
(12) Palacios, D. S., Dailey, I., Siebert, D. M., Wilcock, B. C., and Burke, M. D. (2011) Synthesis-enabled functional group deletions reveal key underpinnings of amphotericin B ion channel and antifungal activities. *Proc. Natl. Acad. Sci. U. S. A. 108*, 6733−6738.
(13) Espada, R., Valdespina, S., Alfonso, C., Rivas, G., Ballesteros, M. P., and Torrado, J. J. (2008) Effect of aggregation state on the toxicity of different amphotericin B preparations. *Int. J. Pharm. 361*, 64−69.
(14) Zielińska, J., Wieczór, M., Bączek, T., Gruszecki, M., and Czub, J. (2016) Thermodynamics and kinetics of amphotericin B self-association in aqueous solution characterized in molecular detail. *Sci. Rep. 6*, 19109.
(15) Huang, W., Zhang, Z., Han, X., Tang, J., Wang, J., Dong, S., and Wang, E. (2002) Ion channel behavior of Amphotericin B in sterol-free and cholesterol or ergosterol-containing supported phosphatidylcholine bilayer model membranes investigated by electrochemistry and spectroscopy. *Biophys. J. 83*, 3245−3255.
(16) Barwicz, J., Christian, S., and Gruda, I. (1992) Effects of the aggregation state of amphotericin B on its toxicity to mice. *Antimicrob. Agents Chemother. 36*, 2310−2315.
(17) Antillon, A., de Vries, A. H., Espinosa-Caballero, M., Falcon-Gonzalez, J. M., Romero, D. F., Gonzalez-Damian, J., Jimenez-Montejo, F. E., Leon-Buitimea, A., Lopez-Ortiz, M., Magaña, R., Marrink, S. J., Morales-Nava, R., Periole, X., Reyes-Esparza, J., Lozada, J. R., Santiago-Angelino, T. M., Gonzalez, M. C. V., Regla, I., Carrillo-Tripp, M., Fernandez-Zertuche, M., Rodriguez-Fragoso, L., and Ortega-Blake, I. (2016) An Amphotericin B derivative equally potent to Amphotericin B and with increased safety. *PLoS One 11*, e0162171.
(18) Mazerski, J., Grzybowska, J., and Borowski, E. (1990) Influence of net charge on the aggregation and solubility behavior of Amphotericin B and its derivatives in aqueous media. *Eur. Biophys. J. 18*, 159−164.
(19) Preobrazhenskaya, M. N., Olsufyeva, E. N., Solovieva, S. E., Tevyashova, A. N., Reznikova, M. I., Luzikovm, Y. N., Terekhova, L. P., Trenin, A. S., Galatenko, O. A., Treshalinm, I. D., Michink, E. P., Bukhman, V. M., Sletta, H., and Zotchev, S. B. (2009) Chemical modification and biological evaluation of new semisynthetic derivatives of 28, 29-didehydronystatin A1 (S44HP), a genetically engineered antifungal polyene macrolide antibiotic. *J. Med. Chem. 52*, 189−196.
(20) Preobrazhenskaya, M. N., Olsufyeva, E. N., Tevyashova, A. N., Printsevskaya, S. S., Solovieva, S. E., Reznikova, M. I., Trenin, A. S., Galatenko, O. A., Treshalin, I. D., Pereverzeva, E. R., Mirchink, E. P., and Zotchev, S. B. (2010) Synthesis and study of the antifungal activity of new mono- and disubstituted derivatives of a genetically engineered polyene antibiotic 28,29-didehydronystatin A1 (S44HP). *J. Antibiot. 63*, 55−64.
(21) Tevyashova, A. N., Olsufyeva, E. N., Solovieva, S. E., Printsevskaya, S. S., Reznikova, M. I., Trenin, A. S., Galatenko, O. A., Treshalin, I. D., Pereverzeva, E. R., Mirchink, E. P., Isakova, E. B., Zotchev, S. B., and Preobrazhenskaya, M. N. (2013) Structure-antifungal activity relationships of polyene antibiotics of the Amphotericin B group. *Antimicrob. Agents Chemother. 57*, 3815−3822.
(22) Paquet, V., and Carreira, E. M. (2006) Significant Improvement of antifungal activity of polyene macrolides by bisalkylation of the mycosamine. *Org. Lett. 8*, 1807−1809.
(23) Endo, M. M., Cioffi, A. G., and Burke, M. D. (2016) Our path to less toxic Amphotericins. *Synlett 27*, 337−354.
(24) Nyberg, N. Y., Duus, J. O., and Sorensen, O. W. (2005) Heteronuclear two-bond correlation: suppressing heteronuclear three-bond or higher NMR correlations while enhancing two-bond correlations even for vanishing $^{2}J_{CH}$. *J. Am. Chem. Soc. 127*, 6154−6155.
(25) Reference method for broth dilution antifungal susceptibility testing of yeasts; approved standard. NCCLS document M27-A [ISBN 1-56238-328-0]. NCCLS, Pennsylvania, USA, 1997.
(26) Reference method for broth dilution antifungal susceptibility testing of filamentous fungi; approved standard. NCCLS document M38-A [ISBN 1-56238-470-8]. NCCLS, Pennsylvania, USA, 2002.
(27) Finkelstein, A., and Cass, A. (1968) Permeability and electrical properties of thin lipid membranes. *J. Gen. Physiol. 52*, 145−172.
(28) Kleinberg, M. E., and Finkelstein, A. (1984) Single-length and double-length channels formed by nystatin in lipid bilayer membranes. *J. Membr. Biol. 80*, 257−269.
(29) Marty, A., and Finkelstein, A. (1975) Pores formed in lipid bilayer membranes by nystatin, Differences in its one-sided and two-sided action. *J. Gen. Physiol. 65*, 515−526.
(30) Brutyan, R. A., and McPhie, P. (1996) On the one-sided action of amphotericin B on lipid bilayer membranes. *J. Gen. Physiol. 107*, 69−78.
(31) Baginski, M., Resat, H., and Borowski, E. (2002) Comparative molecular dynamics simulations of amphotericin B−cholesterol/ergosterol membrane channels. *Biochim. Biophys. Acta, Biomembr. 1567*, 63−78.
(32) Khutorsky, V. E. (1996) Ion coordination in the amphotericin B channel. *Biophys. J. 71*, 2984−2995.
(33) Khutorsky, V. E. (1992) Structures of amphotericin B-cholesterol complex. *Biochim. Biophys. Acta, Biomembr. 1108*, 123−127.
(34) Koch, W., and Holthausen, M. C. (2001) *A chemist's guide to density functional theory*, 2nd ed., p 78, Wiley-VCH Verlag GmbH
(35) Sowiński, P., Pawlak, J., Borowski, E., and Gariboldi, P. (1992) ^{1}H NMR Model studies of Amphotericin B: comparison of X-Ray and NMR stereochemical data. *Magn. Reson. Chem. 30*, 275−279.
(36) Neumann, A., Baginski, M., and Czub, J. (2010) How do sterols determine the antifungal activity of Amphotericin B? Free energy of binding between the drug and its membrane target. *J. Am. Chem. Soc. 132*, 18266−18272.
(37) Chulkov, E. G., Efimova, S. S., Schagina, L. V., and Ostroumova, O. S. (2014) Direct visualization of solid ordered domains induced by polyene antibiotics in giant unilamellar vesicles. *Chem. Phys. Lipids 183*, 204−207.
(38) Efimova, S. S., Schagina, L. V., and Ostroumova, O. S. (2014) Investigation of channel-forming activity of polyene macrolide antibiotics in planar lipid bilayers in the presence of dipole modifiers. *Acta Naturae. 6*, 67−79.
(39) Efimova, S. S., Tevyashova, A. N., Olsufyeva, E. N., Bykov, E. E., and Ostroumova, O. S. (2017) Pore-forming activity of new conjugate antibiotics based on amphotericin B. *PLoS One 12* (11), e0188573.

https://dx.doi.org/10.1021/acsinfecdis.0c00068
ACS Infect. Dis. 2020, 6, 2029−2044

(40) Wang, G., Chang, X., Peng, J., Liu, K., Zhao, K., Yu, C., and Fang, Y. (2015) Towards a new FRET system via combination of pyrene and perylene bisimide: synthesis, self-assembly and fluorescence behavior. *Phys. Chem. Chem. Phys. 17*, 5441−5449.
(41) Matulková, Ia, Solarová, H., Štepnicka, P., Císarová, I., Janda, T., Nemec, P., and Nemec, I. (2015) (2-Azoniaethyl)guanidinium dichloride − A promising phase-matchable NLO material employing a simple hydrogen bond acceptor in its structure. *Opt. Mater. 42*, 39−46.
(42) Montal, M., and Mueller, P. (1972) Formation of bimolecular membranes from lipid monolayers and a study of their electrical properties. *Proc. Natl. Acad. Sci. U. S. A. 69*, 3561−3566.
(43) Ostroumova, O. S., Chulkov, E. G., Stepanenko, O. V., and Schagina, L. V. (2014) Effect of flavonoids on the phase separation in giant unilamellar vesicles formed from binary lipid mixtures. *Chem. Phys. Lipids 178*, 77−83.
(44) Juhasz, J., Davis, J. H., and Sharom, F. J. (2010) Fluorescent probe partitioning in giant unilamellar vesicles of 'lipid raft' mixtures. *Biochem. J. 430*, 415−423.
(45) Spartan Software, https://www.wavefun.com/products/spartan.html (accessed June 11, 2020).
(46) *Council of Europe European convention for the protection of vertebrate animals used for experimental and other scientific purposes*, ETS No. 123, Council of Europe, Strasbourg, 1986.
(47) Directive 2010/63/EU on the protection of animals used for scientific purposes EN. *Official Journal of the European Union*, 2010, L276/33−276/79.
(48) National State Standard GOST P 53434−2009 the Russian Federation standard "The Principles of Good Laboratory Practice" (Approved and Put into Effect by the Order of the Federal Agency for Technical Regulation and Metrology of December 2, 2009), No 544. Available online: http://docs.cntd.ru/document/1200075972 (accessed on 3 March 2010) (In Russian).

https://dx.doi.org/10.1021/acsinfecdis.0c00068
ACS Infect. Dis. 2020, 6, 2029−2044